Report No. UT-14.01

COMPARISON OF WINTER TEMPERATURE PROFILES IN ASPHALT AND CONCRETE PAVEMENTS

Prepared For:

Utah Department of Transportation
Research Division

Submitted By:

Brigham Young University
Department of Civil and Environmental Engineering

Authored By:

W. Spencer Guthrie, Ph.D.
Jeremy B. Dye
Dennis L. Eggett, Ph.D.

Final Report
June 2014

RESEARCH

udot.utah.gov
Utah Department of Transportation - Research Division
4501 South 2700 West - P.O. Box 148410 - SLC,UT 84114-8410

DISCLAIMER

The authors alone are responsible for the preparation and accuracy of the information, data, analysis, discussions, recommendations, and conclusions presented herein. The contents do not necessarily reflect the views, opinions, endorsements, or policies of the Utah Department of Transportation or the US Department of Transportation. The Utah Department of Transportation makes no representation or warranty of any kind, and assumes no liability therefore. The authors make no warranty, express or implied, regarding the suitability of findings documented in this report for a particular purpose and shall not be held liable under any circumstances for any direct, consequential, or other damages with respect to claims by users of any findings documented in this report, including claims based on allegations of errors, omissions, or negligence.

TECHNICAL REPORT DOCUMENTATION

1. Report No. UT-14.01	2. Government Accession No.	3. Recipient's Catalog No.

4. Title and Subtitle COMPARISON OF WINTER TEMPERATURE PROFILES IN ASPHALT AND CONCRETE PAVEMENTS	5. Report Date June 2014
	6. Performing Organization Code
7. Author(s) W. Spencer Guthrie, Jeremy B. Dye, and Dennis L. Eggett	8. Performing Organization Report No.
9. Performing Organization Name and Address Brigham Young University Department of Civil and Environmental Engineering 368 Clyde Building Provo, UT 84602	10. Work Unit No. 8RD1243H
	11. Contract or Grant No. 099087
12. Sponsoring Agency Name and Address Utah Department of Transportation 4501 South 2700 West P.O. Box 148410 Salt Lake City, UT 84114-8410	13. Type of Report & Period Covered Research: May 2009 to August 2010
	14. Sponsoring Agency Code PIC No. UT07.208

15. Supplementary Notes

Research performed in cooperation with the Utah Department of Transportation.

16. Abstract

The objectives of this research were to 1) determine which pavement type, asphalt or concrete, has higher surface temperatures in winter and 2) compare the subsurface temperatures under asphalt and concrete pavements to determine the pavement type below which more freeze-thaw cycles of the underlying soil occur. For analysis, 12 continuous months of climatological data primarily from the 2009 calendar year were acquired from 22 environmental sensor stations (ESSs) near asphalt roads and nine ESSs near concrete roads. To predict pavement surface temperature, a multiple linear regression was performed with input parameters of pavement type, time period, and air temperature. Similarly, a multiple linear regression was performed to predict the number of subsurface freeze-thaw cycles, based on month, latitude, elevation, and pavement type. A finite-difference model was created to model surface temperatures of asphalt and concrete pavements based on air temperature and incoming radiation.

With respect to pavement surface temperatures, the results showed that, for near-freezing conditions, asphalt is warmer during the afternoon and concrete is warmer during other times of the day, but that neither pavement type is warmer, on average. The regression equation predicting the number of subsurface freeze-thaw cycles provided estimates that did not correlate well with measured values; data that were not available for this research but are likely necessary in estimating the number of freeze-thaw cycles under the pavement include pavement layer thicknesses, layer types, and layer moisture contents.

17. Key Words Asphalt Concrete, Environmental Sensor Station, Freeze-Thaw Cycles, Pavement Temperature Profiles, Portland Cement Concrete, Road Weather Information System, Winter Maintenance		18. Distribution Statement Available: Not restricted. Available through: UDOT Research Division 4501 South 2700 West P.O. Box 148410 Salt Lake City, UT 84114-8410 www.udot.utah.gov/go/research		23. Registrant's Seal
19. Security Classification (of this report) Unclassified	20. Security Classification (of this page) Unclassified	21. No. of Pages 88	22. Price	

ACKNOWLEDGMENTS

The authors acknowledge the Utah Department of Transportation for funding this research.

TABLE OF CONTENTS

LIST OF TABLES xi
LIST OF FIGURES xiii
LIST OF ACRONYMS xv
EXECUTIVE SUMMARY xvii
1.0 INTRODUCTION 1
  1.1 Problem Statement 1
  1.2 Scope 2
  1.3 Outline of Report 3
2.0 BACKGROUND 5
  2.1 Overview 5
  2.2 Thermal Properties of Asphalt and Concrete 5
    2.2.1 Albedo 5
    2.2.2 Specific Heat 6
    2.2.3 Thermal Conductivity 6
  2.3 Daily Temperature Trends 7
  2.4 Road Weather Information Systems 7
    2.4.1 Atmospheric Sensors 10
    2.4.2 Pavement Sensors 13
  2.5 Summary 15
3.0 PROCEDURES 17
  3.1 Overview 17
  3.2 Data Acquisition 17
    3.2.1 Road Weather Information System Data 17
    3.2.2 Pavement Type 18
  3.3 Data Management 24

3.3.1 Removal of Incorrect or Unnecessary Data 24
3.3.2 Division of Data into Time Periods 25
3.3.3 Calculation of Monthly Freeze-Thaw Cycles 28
3.4 Statistical Analyses 29
3.4.1 Pavement Surface Temperatures... 30
3.4.2 Subsurface Freeze-Thaw Cycles 30
3.5 Finite-Difference Modeling 31
3.6 Summary.. 34
4.0 RESULTS 35
4.1 Overview.. 35
4.2 Statistical Analyses 35
4.2.1 Pavement Surface Temperatures.. 35
4.2.2 Subsurface Freeze-Thaw Cycles 45
4.3 Finite-Difference Modeling 50
4.4 Summary... 53
5.0 CONCLUSION... 55
5.1 Summary... 55
5.2 Findings 56
5.2.1 Pavement Surface Temperatures.. 56
5.2.2 Subsurface Freeze-Thaw Cycles 57
5.3 Recommendations... 57
REFERENCES 59
APPENDIX: Division of Data into Time Periods Based on Road Temperatures 63

LIST OF TABLES

Table 3.1 MesoWest Stations with Road Weather Data 18

Table 3.2 Pavement Type and Date Range for All Available Stations 21

Table 3.3 Description of Time Periods...26

Table 3.4 Time Periods for Late Morning, Early Afternoon, Evening, Night, and Early Morning Based on Month 27

Table 3.5 Material Properties Used in Finite-Difference Model..................................33

Table 4.1 Regression Equations for Pavement Surface Temperatures..........................36

Table 4.2 Results of Statistical Analyses for Prediction of Pavement Surface Temperatures...43

Table 4.3 Air Temperatures Corresponding to Freezing Pavement Surface Temperatures...44

Table 4.4 Results of Statistical Analyses for Predicting Subsurface Freeze-Thaw Cycles...48

LIST OF FIGURES

Figure 2.1 Environmental Sensor Station near Centerville, Utah....................................8
Figure 2.2 Radiation Shield Surrounding Thermometer and Hygrometer 11
Figure 2.3 Windmill Anemometer..11
Figure 2.4 Precipitation Occurrence Sensor 12
Figure 2.5 Pavement Sensor near Soldier Summit, Utah...14
Figure 3.1 Google Street View Showing Asphalt Pavement at Station UT28 19
Figure 3.2 Google Street View Showing Concrete Pavement at Station UTMFS 19
Figure 3.3 RWIS Stations on Asphalt Roads...22
Figure 3.4 RWIS Stations on Concrete Roads...23
Figure 3.5 Typical Pavement Surface Temperatures for Each Time Period 28
Figure 3.6 Schematic of Finite-Difference Model 33
Figure 4.1 Predicted Pavement Surface Temperatures for Late Morning 37
Figure 4.2 Predicted Pavement Surface Temperatures for Early Afternoon 38
Figure 4.3 Predicted Pavement Surface Temperatures for Late Afternoon....................39
Figure 4.4 Predicted Pavement Surface Temperatures for Evening 40
Figure 4.5 Predicted Pavement Surface Temperatures for Night 41
Figure 4.6 Predicted Pavement Surface Temperatures for Early Morning.....................42
Figure 4.7 Number of Subsurface Freeze-Thaw Cycles versus Month 46
Figure 4.8 Number of Monthly Subsurface Freeze-Thaw Cycles versus Elevation.......46
Figure 4.9 Number of Monthly Subsurface Freeze-Thaw Cycles versus Latitude.........47
Figure 4.10 Number of Monthly Subsurface Freeze-Thaw Cycles versus Longitude 47
Figure 4.11 Predicted versus Observed Number of Subsurface Freeze-Thaw Cycles 50
Figure 4.12 Temperature Profiles Reflecting a 1°C Increase in Air Temperature 51
Figure 4.13 Temperature Profiles Reflecting a 1°C Increase in Air Temperature and 100 W/m^2 Incident Radiation 52

LIST OF ACRONYMS

ESS	Environmental Sensor Station
FHWA	Federal Highway Administration
ID	Identification Number
RWIS	Road Weather Information Systems
UDOT	Utah Department of Transportation

EXECUTIVE SUMMARY

Because winter maintenance is so costly, Utah Department of Transportation (UDOT) personnel asked researchers at Brigham Young University to determine whether asphalt or concrete pavements require more winter maintenance. Differing thermal properties suggest that, for the same environmental conditions, asphalt and concrete pavements will have different temperature profiles. Climatological data from 22 environmental sensor stations (ESSs) near asphalt roads and nine ESSs near concrete roads were used to 1) determine which pavement type has higher surface temperatures in winter and 2) compare the subsurface temperatures under asphalt and concrete pavements to determine the pavement type below which more freeze-thaw cycles of the underlying soil occur.

Twelve continuous months of climatological data, primarily from the 2009 calendar year, were acquired from the road weather information system operated by UDOT, and erroneous data were removed from the data set. To predict pavement surface temperature, a multiple linear regression was performed with input parameters of pavement type, time period, and air temperature. Similarly, a multiple linear regression was performed to predict the number of subsurface freeze-thaw cycles, based on month, latitude, elevation, and pavement type. A finite-difference model was created to model surface temperatures of asphalt and concrete pavements based on air temperature and incoming radiation.

The statistical analysis predicting pavement surface temperatures showed that, for near-freezing conditions, asphalt is better in the afternoon, and concrete is better for other times of the day, but that neither pavement type is better, on average. Asphalt and concrete are equally likely to collect snow or ice on their surfaces, and both pavements are expected to require equal amounts of winter maintenance, on average. Finite-

difference analysis results confirmed that, for times of low incident radiation (night), concrete reaches higher temperatures than asphalt, and, for times of high incident radiation (day), asphalt reaches higher temperatures than concrete.

The regression equation predicting the number of subsurface freeze-thaw cycles provided estimates that did not correlate well with measured values. Consequently, an entirely different analysis must be conducted with different input variables. Data that were not available for this research but are likely necessary in estimating the number of freeze-thaw cycles under the pavement include pavement layer thicknesses, layer types, and layer moisture contents.

1.0 INTRODUCTION

1.1 Problem Statement

The Utah Department of Transportation (UDOT) is responsible for the winter maintenance of 26,184 lane-kilometers (16,270 lane-miles) of state highways (*1*), which is a significant undertaking because Utah has an average of about 25 snowstorms each year. Consequently, winter maintenance is very expensive. For example, in 2009, UDOT spent approximately $22 million on snow removal (*2*). In this research, the term *winter maintenance* is used to describe all maintenance activities attributed to winter weather. Winter maintenance includes identifying and removing snow and ice from the road surface through snowplows, sand, and salt.

Because winter maintenance is so costly, UDOT personnel recognized the need for research on winter maintenance and asked researchers at Brigham Young University to determine whether asphalt or concrete pavements require more winter maintenance. In the past, engineers have typically considered factors such as construction cost, duration of construction, strength requirements, ride quality, and safety when selecting pavement type. However, winter maintenance costs have not been considered in life-cycle cost analyses appropriately performed in the decision-making process (*3*). Furthermore, while researchers have studied how asphalt pavements react to surface weather by predicting pavement surface temperatures from weather data, asphalt and concrete pavements have not been directly compared (*4, 5*). Similarly, although researchers have also created computer models to predict maximum asphalt pavement surface temperatures from environmental data, the scope of that work did not include investigations of different pavement types (*6*). Consequently, because no studies have compared the winter maintenance requirements of asphalt and concrete pavements, the ideal pavement type to select based on winter maintenance is not known.

Besides the immediate costs of snowplows, sanding, and salting, winter maintenance also includes needed pavement repairs caused by winter weather. Every spring, thousands of potholes caused by winter weather must be patched (*7*). Subsurface freeze-thaw cycles contribute to the deterioration of the pavement, both through differential heaving and through cyclic expansion and contraction (*8*). Freeze-thaw damage can be manifest as cracking and surface roughness in affected pavements (*9*). Knowing how the pavement type affects subsurface freezing and thawing can help engineers predict secondary winter maintenance costs for each pavement type. Previous research has led to guides that predict frost penetration through asphalt and concrete pavements into the underlying subgrade (*10*), but no studies have been published that compare the number of freeze-thaw cycles that occur beneath asphalt and concrete pavements.

This research investigated the winter maintenance costs of asphalt and concrete through two main objectives. The first objective was to establish the difference in surface temperatures between asphalt and concrete pavements for the same climatic conditions. This knowledge will help engineers predict which pavement type will require more winter maintenance costs in terms of snow removal and salting. The second objective was to compare the subsurface temperatures under asphalt and concrete pavements to determine the pavement type below which more freeze-thaw cycles of the underlying soil occur. This knowledge will help engineers decide which pavement type should be used for regions with frost-susceptible subgrades.

1.2 Scope

The climatological data used in this report were obtained from 31 environmental sensor stations (ESSs) in Utah. The data were used to compare the cold-weather pavement surface temperatures of nine concrete pavements and 22 asphalt pavements in Utah, accounting for climatic factors such as air temperature, wind speed, and precipitation as well as geographical factors such as elevation, latitude, and longitude. This report also compares the temperatures 45 cm (18 in.) below those same pavements to analyze the numbers of freeze-thaw cycles that occur under asphalt and concrete pavements during the course of one year.

All highly-traveled roads in Utah have at least one ESS, so the data from this report are generally representative of major roadways in Utah. The elevations range from 1,285 m to 3192 m (4,215 ft to 10,472 ft), latitudes range from 37.48° to 41.91°, and longitudes range from −110.49° to −113.64°.

1.3 Outline of Report

This report contains five chapters. Chapter 1 presents the objectives and scope of the research. Chapter 2 gives background on thermal properties of asphalt and concrete pavements as well as daily temperature trends. It also gives background on road weather information systems (RWIS) and the different instruments used to collect weather data. Chapter 3 details the procedures used for data acquisition and data reduction. It also explains the procedures used to create a finite-difference model and set up two statistical analyses. Chapter 4 provides the results of the statistical analyses and the finite-difference model and a discussion of the findings. Chapter 5 summarizes the major findings of the research and recommends how transportation engineers can incorporate the findings into future decision-making.

2.0 BACKGROUND

2.1 Overview

This chapter provides a theoretical basis for why asphalt and concrete pavements should have different surface temperatures, based on differing thermal properties of asphalt and concrete. It also explains what an RWIS is and how it collects climatological data.

2.2 Thermal Properties of Asphalt and Concrete

Engineers have long known that temperature plays an important role in the performance of pavement structures. Evidences of this include rutting of asphalt pavements at high temperatures when appropriate asphalt binders are not selected (*11*), cracking due to thermally induced expansion and contraction (*12*, *13*), and curling of concrete slabs due to vertical temperature gradients (*14*, *15*). However, no research has explored how asphalt and concrete react differently to the same weather conditions, specifically how pavement surface and subsurface temperatures vary in winter. Asphalt and concrete behave differently because they have very different thermal properties from each other. Three important thermal properties are albedo, specific heat, and thermal conductivity.

2.2.1 Albedo

Latin for *whiteness*, albedo is a measure of how much incoming solar radiation is reflected back into the atmosphere. An albedo of 0.0 means that zero percent of the incoming radiation is reflected back into the atmosphere, while an albedo of 1.0 means that 100 percent of the incoming radiation is reflected back. New asphalt pavements have an albedo of 0.04 to 0.05, while asphalt pavements older than 5 years have an average albedo of about 0.12. Concrete pavements have an albedo of about 0.33, which remains relatively constant for the life of the pavement (*16*).

2.2.2 Specific Heat

Specific heat is a measure of how much energy is necessary to increase the temperature of a given volume of material by one temperature unit as defined in Equation 2.1:

$$c = \frac{Q}{V \cdot \Delta T} \tag{2.1}$$

where c = specific heat (J $\mathrm{m^{-3}}$ $\mathrm{°C^{-1}}$)

Q = energy entering the pavement (J)

V = volume of pavement ($\mathrm{m^3}$)

ΔT = average increase in temperature (°C)

The specific heat of concrete is around 2.07 J $\mathrm{cm^{-3}}$ $\mathrm{°C^{-1}}$, while the value for asphalt is 1.42 J $\mathrm{cm^{-3}}$ $\mathrm{°C^{-1}}$ (*17*). Thus, roughly 1.45 times as much thermal energy is needed to increase the temperature of a concrete sample than is needed to increase the temperature of an equal volume of asphalt by the same amount.

2.2.3 Thermal Conductivity

Thermal conductivity is a measure of how quickly heat is transferred through the material as defined in Equation 2.2:

$$P = k\frac{\Delta T}{\Delta h}A \tag{2.2}$$

where: P = thermal energy transferred from one layer of pavement to the next (W)

k = thermal conductivity (W $\mathrm{m^{-1}}$ $\mathrm{°C^{-1}}$)

ΔT = difference in temperature across h (°C)

Δh = thickness of layer (m)

A = area of pavement normal to direction of heat flow (m^2)

The thermal conductivity values for asphalt and concrete are 0.74 $W\ m^{-1}\ °C^{-1}$ and 1.69 $W\ m^{-1}\ °C^{-1}$, respectively (*17*). Thus, concrete has approximately 2.3 times the thermal conductivity of asphalt, meaning that heat from the surface of a concrete pavement propagates into the pavement faster than it does through asphalt.

2.3 Daily Temperature Trends

Through the course of a day, the pavement surface temperature is always changing. After the sun rises, incoming solar radiation heats the earth's atmosphere, causing the air temperature to rise. At the same time, solar radiation reaches the pavement surface, causing the surface temperature to increase. Thus, the two main mechanisms for heat transfer into the pavement are convection from the air (a function of thermal conductivity and specific heat) and radiation from the sun and air (a function of albedo and specific heat). Additionally, heat stored from the previous day (a function of thermal conductivity and specific heat) is conducted upwards from the underlying layers. All of these factors combine to determine the current temperature of the pavement.

As the day progresses, the pavement temperature reaches a maximum value a couple of hours after noon and then decreases quickly until nightfall, at which point it continues slowly decreasing until sunrise. Logically, the temperature difference between asphalt and concrete would not be the same at all times of the day because one pavement might heat up faster, leading to a higher high, and cool down faster, leading to a lower low.

2.4 Road Weather Information Systems

To help identify locations that need winter maintenance, UDOT personnel rely on an extensive network of ESSs that monitor key weather data. Figure 2.1 shows a typical

ESS in Utah. Data from the individual ESSs are combined to form an RWIS. Collected data include air temperature, wind speed and direction, presence of precipitation, and visibility. In all, 73 ESSs have been installed across Utah (*18*).

ESSs are sold by approximately 44 companies in the United States (*19*). While each company has a different product or combination of products, most companies offer ESSs that record the same basic weather data. However, when purchasing an ESS, the customer can choose which instruments to install at each location. For this reason, some ESSs collect more information than others.

As part of the RWIS network, several of the ESSs have sensors, often called pucks, embedded in the surface of the road. These sensors measure the pavement surface

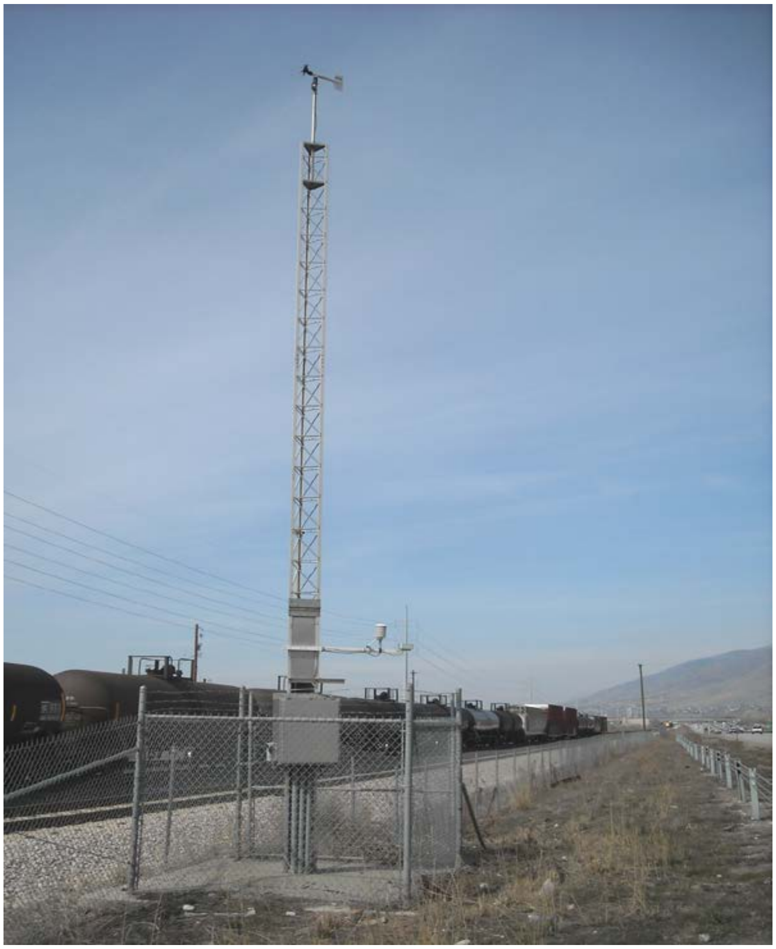

Figure 2.1 Environmental sensor station near Centerville, Utah.

temperature, the presence and depth of moisture on the surface, and the quantity of salts in the surface water. Additionally, many pucks are installed with a subsurface temperature probe that measures the temperature 45 cm (18 in.) underground. Because the pucks are relatively expensive and because they require significant upkeep, only about 30 ESSs in Utah have working pucks (*18*). For most ESSs, the tower is typically located about 9 to 15 m (30 to 50 ft) from the edge of the road (*20*), and the puck is embedded in the surface of the pavement, usually just outside of the outside wheel path (*21*).

The primary purposes of the RWIS are to observe and to predict the drivability of Utah's roads as affected by winter weather (*22*). These stations have all but eliminated the need for individuals to patrol the major roads looking for locations that need winter maintenance (*20*). Instead, the RWIS helps UDOT personnel predict winter storms, and it provides immediate feedback to engineers so that snowplows can be sent to affected areas before snow or ice has rendered the road impassable. Consequently, an increasing number of roads are kept open and safe for more days of the year.

A secondary objective of the RWIS is to help inform the traveling public of upcoming weather conditions so drivers can take alternate routes or plan for slower driving conditions (*22*). UDOT has created a website called CommuterLink that displays traffic accidents, road construction, and weather information to "make driving in Utah more efficient and less frustrating" (*23*).

A tertiary purpose of the RWIS is to facilitate research focused on interactions between pavement systems and environmental conditions. Through research, winter maintenance may not only be predicted but also reduced. With the necessary knowledge, a pavement type could be selected that would perform better in winter weather, reducing the winter maintenance requirements.

The following sections describe several of the most common instruments used in ESSs. At UDOT installations, measurements are usually taken every 10 minutes and transmitted wirelessly to a UDOT server.

2.4.1 Atmospheric Sensors

Atmospheric sensors are attached to the ESS tower and monitor surface weather close to the road. They are typically located a short distance from the road to prevent interference from vehicles. The most common atmospheric sensors measure air temperature, relative humidity, dew point, wind speed and direction, precipitation, solar radiation, visibility, and barometric pressure (*21*).

2.4.1.1 Air Temperature, Relative Humidity, and Dew Point

Air temperature is measured by a thermometer housed in a cylindrical radiation shield mounted on the side of the ESS. The radiation shield allows for an accurate measure of air temperature independent of solar radiation. A hygrometer, used to measure relative humidity, is also housed in the same enclosure, and the combination of air temperature and relative humidity is used to determine dew point (*24*). Figure 2.2 shows a radiation shield surrounding the thermometer and hygrometer.

2.4.1.2 Wind Speed and Direction

The most common devices used in ESSs to measure wind are windmill anemometers, shown in Figure 2.3. Average wind speed, maximum wind speed, and wind direction are reported for each time increment.

2.4.1.3 Precipitation

Several different types of devices measure precipitation, and an ESS could have any one of them or none at all. A precipitation-occurrence sensor, shown in Figure 2.4, outputs either *yes* or *no*, indicating whether or not precipitation is occurring. An optical weather identifier classifies the type, intensity, and rate of precipitation (*24*).

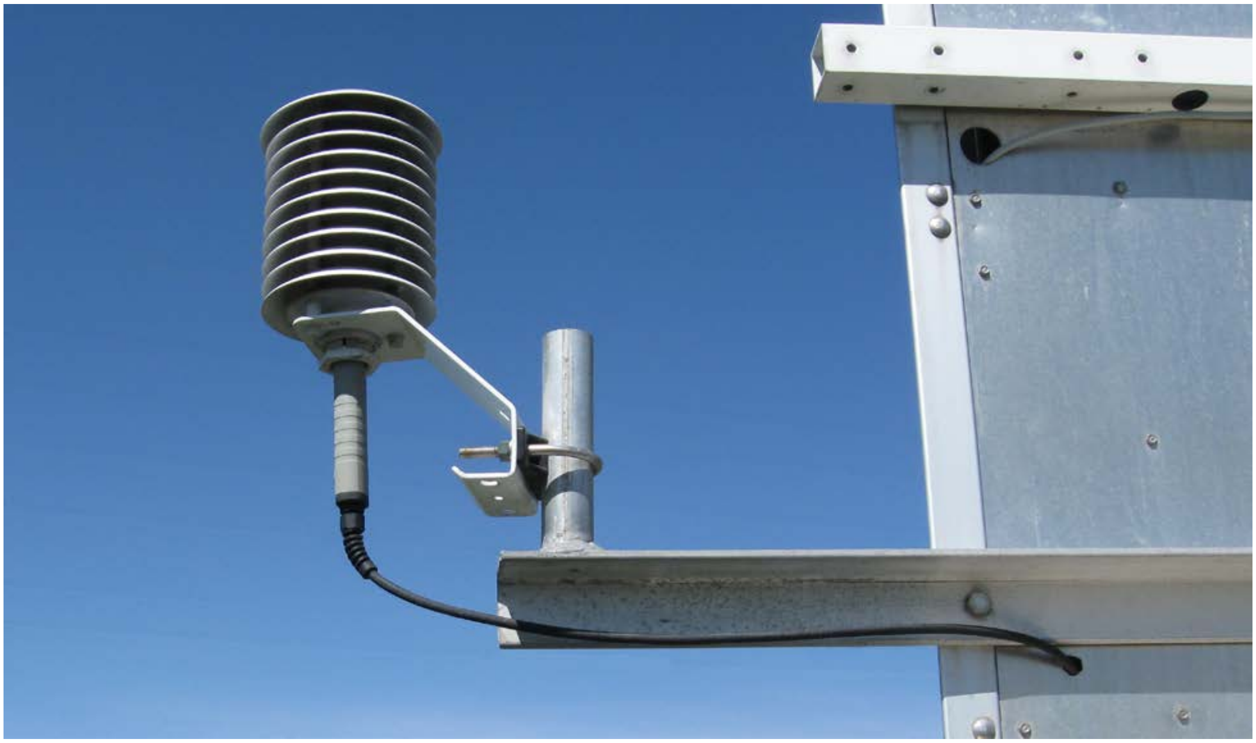

Figure 2.2 Radiation shield surrounding thermometer and hygrometer.

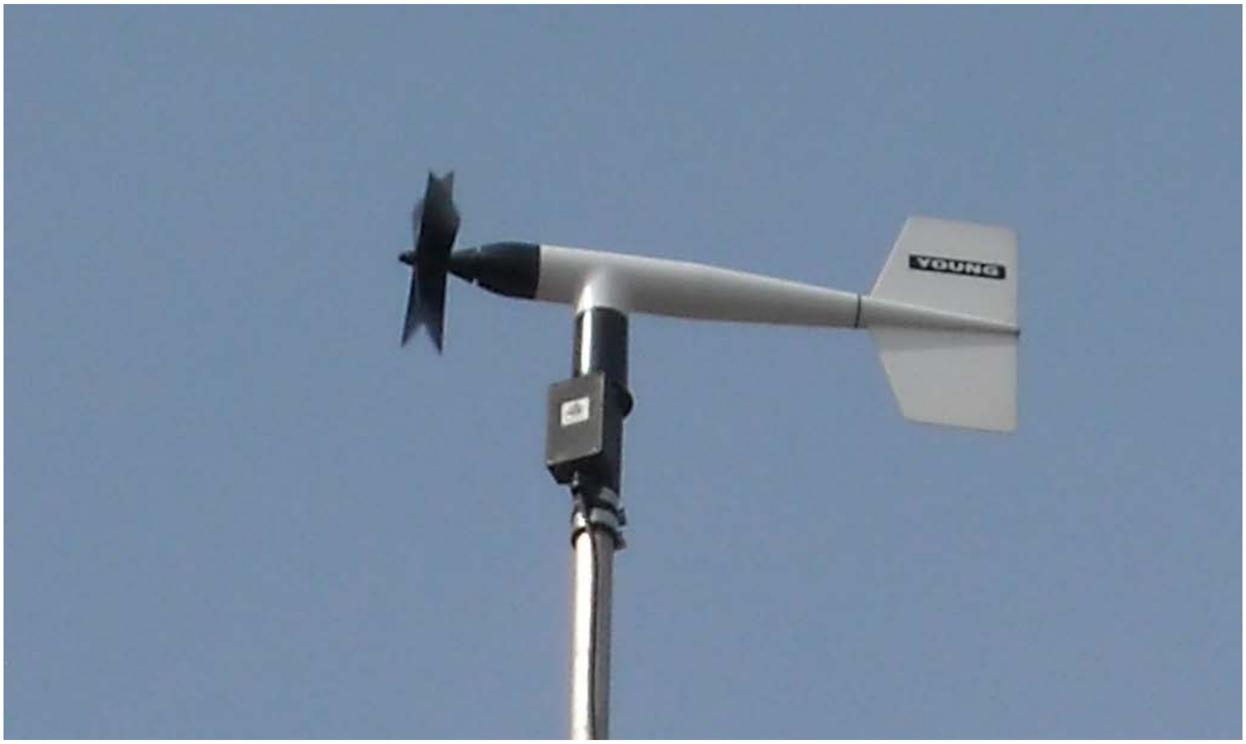

Figure 2.3 Windmill anemometer.

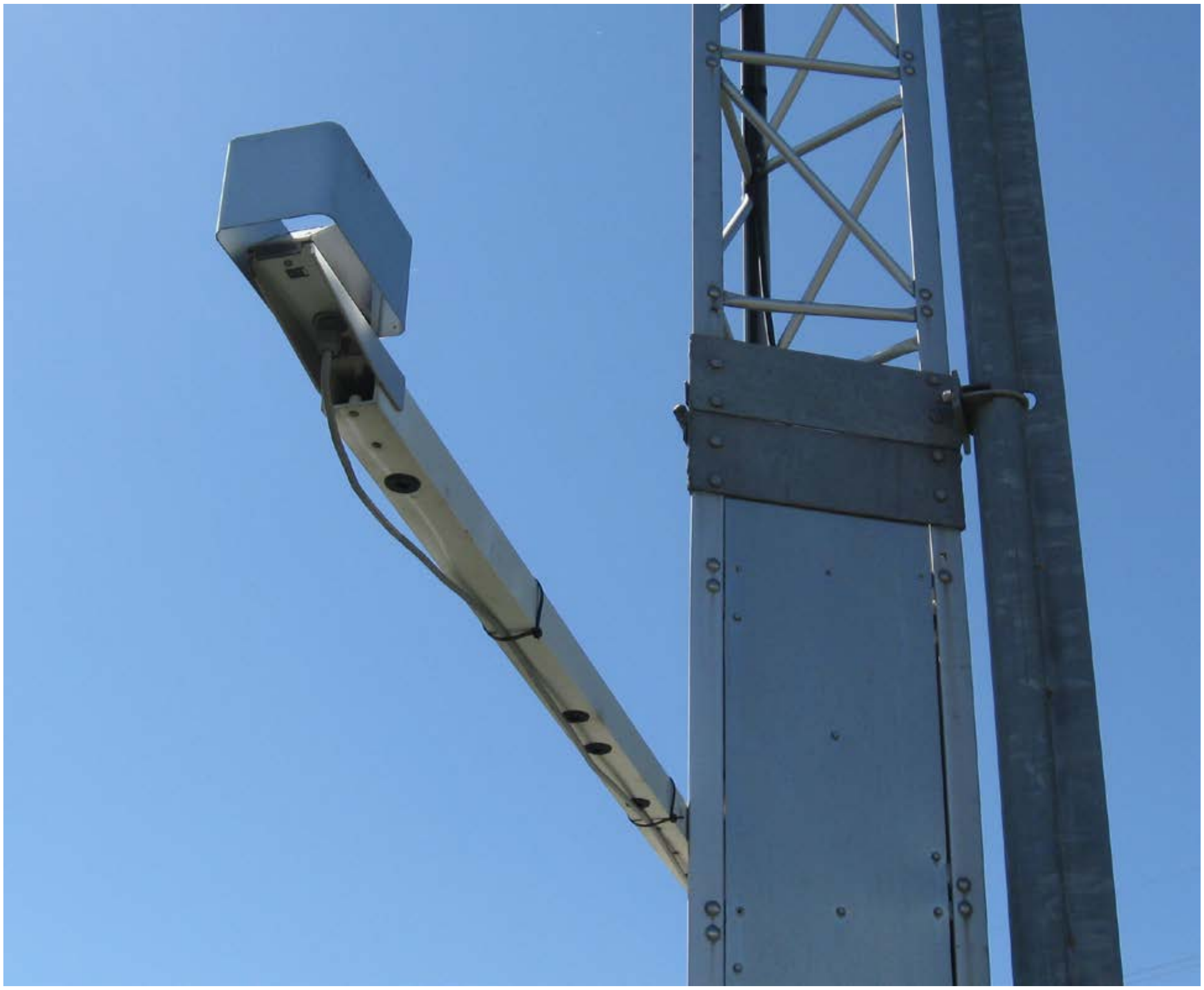

Figure 2.4 Precipitation occurrence sensor.

2.4.1.4 Solar Radiation

Solar radiation is measured by pyranometers, which detect both diffused and direct solar radiation. The pyranometers are typically small hemispheres pointed upward that measure radiation incident to a plane (*25*).

2.4.1.5 Visibility

Visibility is measured by a technique called forward scatter, in which light is projected towards a sensor. Particulates in the air scatter some of the light, and the sensor detects how much light was not scattered (*24*). Visibility is measured in kilometers (miles) and represents how far a driver can see clearly.

2.4.1.6 Barometric Pressure

Barometers housed in the ESS measure barometric pressure, which is widely used in predicting the onset of stormy weather. The barometer is usually located at the base of the ESS inside the cabinet that houses the data loggers and processing hardware.

2.4.2 Pavement Sensors

Several styles of pavement sensors are available on the market, three of which are available through Vaisala (*26*). Figure 2.5 shows one type of pavement sensor used in Utah. Pavement sensors measure surface temperature, subsurface temperature, presence and depth of moisture on the surface, and quantity of salts in the surface water (*21*).

2.4.2.1 Pavement Surface Temperature

Thermometers embedded in the surface of the pavement measure pavement surface temperature. Pavement surface temperature is an important indicator of whether or not precipitation will freeze on the surface of the road.

2.4.2.2 Subsurface Temperature

Subsurface temperature probes, called thermisters, extend approximately 45 cm (18 in.) below the surface of the pavement, often into the subgrade. The Federal Highway Administration (FHWA) recommends that, for ease of maintenance, subsurface temperature probes not be located directly under the pavement sensor (*21*), but temperature probes in Utah are often placed beneath the pucks so that only one hole needs to be drilled through the wearing course.

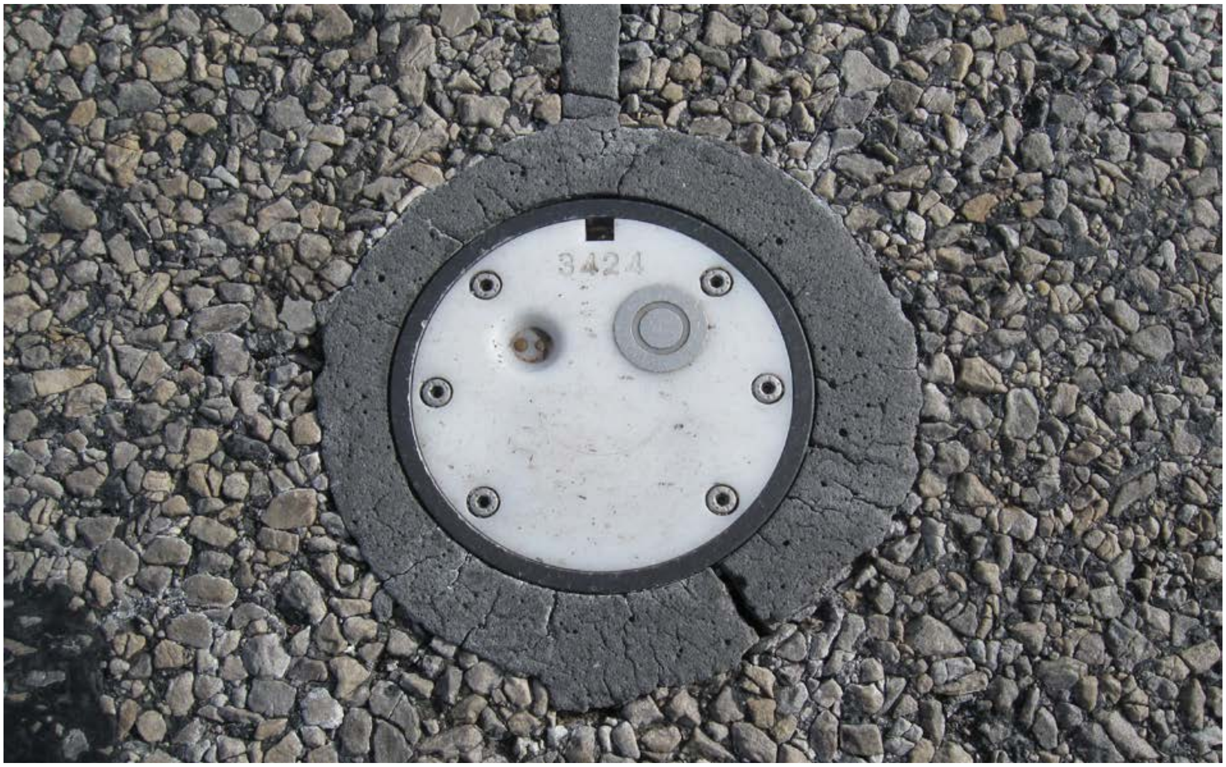

Figure 2.5 Pavement sensor near Soldier Summit, Utah.

2.4.2.3 Presence and Depth of Moisture on the Surface

For detecting moisture on the pavement surface, the two metal rings on the upper right portion of the pavement sensor shown in Figure 2.5 emit multiple frequencies of radar. The radar is used to calculate the amount of moisture, measured in millimeters (inches), on the surface of the pavement (*27*).

2.4.2.4 Quantity of Salts in the Surface Water

For assessment of the quantity of salts in the water on the pavement surface, the pucks use a technology called active sensing. This technique involves cooling of the surface moisture that collects in the small well in the surface of the pavement sensor shown in Figure 2.5 to determine the freezing point of water on the pavement surface. The freezing point is then used to back-calculate the amount of salt on the surface.

Because liquid water is needed for active sensing, the quantity of salts in the surface water can only be determined when the pavement surface is wet (*26*).

2.5 Summary

Differing thermal properties between asphalt and concrete suggest that, for the same environmental conditions, asphalt and concrete pavements will have different temperature profiles. Asphalt typically has a lower albedo than concrete, indicating that asphalt will absorb a larger percentage of incident solar radiation than concrete. Asphalt has a lower specific heat than concrete, meaning that less thermal energy is needed to increase the temperature of asphalt than concrete. Additionally, asphalt has a lower thermal conductivity than concrete, meaning that heat moves more slowly through asphalt pavement than through concrete pavement, all other factors held constant.

Depending on material properties and environmental conditions, asphalt and concrete pavements exhibit changing temperature profiles coinciding to a large degree with the daily solar cycle. In general, a pavement begins heating up shortly after sunrise. As the day progresses, the pavement temperature reaches a maximum a couple of hours after noon and then decreases quickly until nightfall, at which point it continues slowly decreasing until sunrise.

The RWIS operated by UDOT is comprised of 73 ESSs, of which approximately 30 have working pavement sensors. ESSs can be equipped to measure and record the following atmospheric data: air temperature, relative humidity, dew point, wind speed and direction, precipitation, solar radiation, visibility, and barometric pressure. Additionally, pavement sensors measure pavement surface temperature, subsurface temperature, presence and depth of moisture on the surface, and quantity of salts in the surface water.

3.0 PROCEDURES

3.1 Overview

This chapter describes the methods by which the data processed for this research were acquired and organized. It then outlines how the statistical analyses were performed and how a simple finite-difference model was created.

3.2 Data Acquisition

Data from two sources had to be combined into a single database for this research. The following sections detail how RWIS data and pavement type data were acquired.

3.2.1 Road Weather Information System Data

Road weather data for the state of Utah were obtained from MesoWest (*18*). Twelve months of data were downloaded one month at a time for each station, giving a total of almost 400 files, which were later compiled into a single spreadsheet. Table 3.1 shows the Utah stations that have road weather data, their MesoWest identification numbers (IDs), and their locations.

Table 3.1 MesoWest Stations with Road Weather Data

MesoWest ID	Station Name	Elevation, m (ft)	Latitude	Longitude
BAC	Baccus/SR-111	1,576 (5,172)	40.63	−112.05
BHCU1	Brian Head 2S	3,192 (10,472)	37.66	−112.84
CCS	Clear Creek Summit	2,165 (7,103)	38.59	−112.49
CEN	Centerville	1,286 (4,220)	40.95	−111.89
FRE	Fremont Junction	2,073 (6,801)	38.76	−111.38
GHO	Ghost Rocks	2,158 (7,080)	38.86	−110.81
KCWU1	King Canyon	1,915 (6,283)	39.07	−113.64
RTB	Rattlesnake Bench	2,012 (6,601)	38.90	−110.57
SWH	Sherwood Hills	1,725 (5,658)	41.59	−111.97
UT3	Parleys Summit	2,146 (7,040)	40.75	−111.62
UT5	Mouth Parleys	1,498 (4,915)	40.71	−111.80
UT7	Bluffdale	1,433 (4,700)	40.48	−111.90
UT9	Lake Point I-80	1,311 (4,301)	40.69	−112.26
UT11	9000 S/I-15 NB	1,343 (4,407)	40.59	−111.90
UT12	I-15/I-215 SB	1,343 (4,407)	40.64	−111.90
UT21	I-15 @ 600S	1,292 (4,239)	40.75	−111.91
UT28	I-15 @ Tremonton	1,309 (4,295)	41.69	−112.16
UT29	I-15 @ Plymouth	1,370 (4,495)	41.89	−112.17
UT248	SR-248	2,103 (6,900)	40.63	−111.38
UTBLK	I-15 @ Black Ridge	1,573 (5,160)	37.48	−113.22
UTCKH	Chaulk Hill	1,571 (5,155)	41.91	−112.61
UTDOG	Dog Valley	1,884 (6,180)	38.64	−112.61
UTHEB	US-40 Heber	1,747 (5,733)	40.56	−111.43
UTICS	Indian Canyon Summ	2,758 (9,050)	39.89	−110.75
UTLGP	Legacy Parkway	1,285 (4,215)	40.91	−111.91
UTMFS	US-40 Mayflower Su	2,112 (6,929)	40.65	−111.46
UTQRY	Parleys Canyon @ Q	1,554 (5,100)	40.73	−111.77
UTR20	UT-20	2,411 (7,910)	38.03	−112.53
UTSCI	I-15 @ Scipio Summ	1,817 (5,960)	39.20	−112.17
UTSLD	Soldier Summit	2,282 (7,487)	39.93	−111.08
UTSTV	US-40 @ Starvation	1,743 (5,720)	40.17	−110.49

3.2.2 Pavement Type

Because the pavement type was not recorded with the ESS data, this information had to be acquired elsewhere. The Street View option of Google Maps was used to locate the ESS and visually identify the pavement type (*28*). Figures 3.1 and 3.2 show two examples of ESSs in Google Street View and whether the pavement is asphalt or concrete.

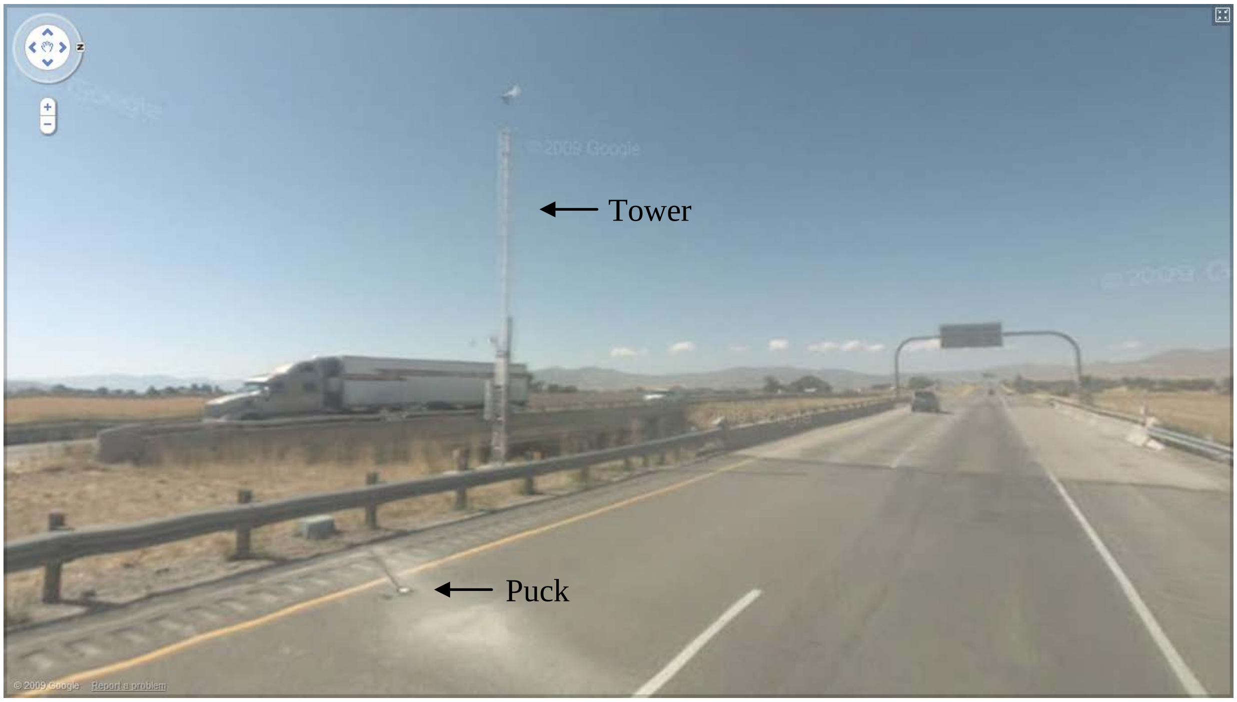
Tower
Puck
© 2009 Google
Report a problem

Figure 3.1 Google Street View showing asphalt pavement at station UT28 (*28*).

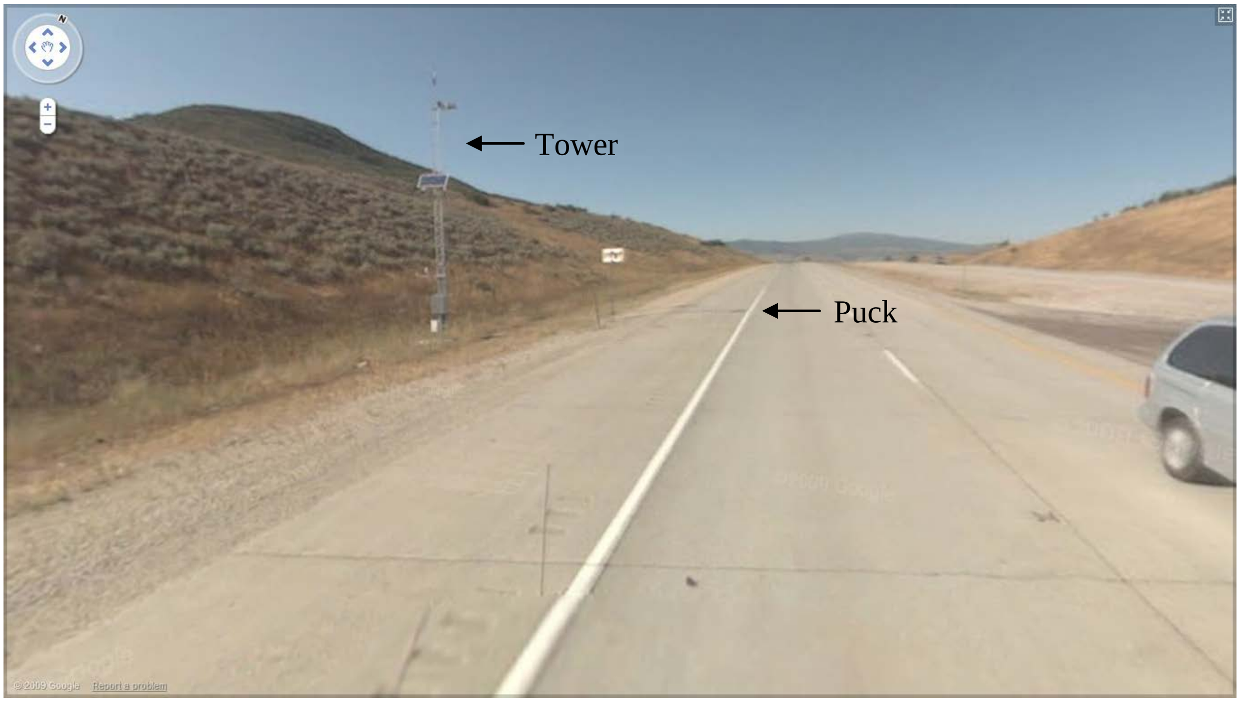
Tower
Puck
© 2009 Google
Report a problem

Figure 3.2 Google Street View showing concrete pavement at station UTMFS (*28*).

Unfortunately, not all of the ESSs could be located in Google Maps. Of the 32 stations, only 24 were positively identified. Seven of the remaining eight stations had asphalt for several miles in either direction, so these stations were assumed to be located on an asphalt road. The remaining station, UTCKH, was excluded from the data set because of a recent asphalt overlay on top of concrete, so it could not be classified as uniquely asphalt or concrete. Asphalt overlays can often be identified through reflection cracking from the underlying concrete joints.

An additional complication was that not all of the stations had functioning pavement sensors for 2009. Only five concrete pavements had puck data for 2009, and all of them were located in Salt Lake County. Since the desired scope of analysis was the whole state of Utah, additional concrete stations had to be located and added to the database prepared for this research. For each of these concrete stations for which data were not available in 2009, the most recent 12 months of consecutive data were used so that all ESS stations situated on a concrete road and instrumented with a puck were included in the analyses, even if they were not functioning in 2009. For example, the puck at station CCS, which is located on I-70, a concrete road, ceased functioning in early 2008, so no data were available from 2009. However, good data were available from January 2007 to December 2007, so that date range was used instead.

Table 3.2 shows the pavement type and date range for all stations analyzed in this research. The locations are displayed graphically for asphalt and concrete roads in Figures 3.3 and 3.4, which show that asphalt pavements are much more prevalent in Utah than concrete pavements.

Table 3.2 Pavement Type and Date Range for All Available Stations

MesoWest ID	Pavement	Date Range
BAC	Asphalt	Jan 2009 - Dec 2009
BHCU1	Asphalt	Jan 2009 - Dec 2009
FRE	Asphalt	Jan 2009 - Dec 2009
GHO	Asphalt	Jan 2009 - Dec 2009
KCWU1	Asphalt	Jan 2009 - Dec 2009
RTB	Asphalt	Jan 2009 - Dec 2009
SWH	Asphalt	Jan 2009 - Dec 2009
UT3	Asphalt	Jan 2009 - Dec 2009
UT5	Asphalt	Jan 2009 - Dec 2009
UT9	Asphalt	Jan 2009 - Dec 2009
UT28	Asphalt	Jan 2009 - Dec 2009
UT248	Asphalt	Jan 2009 - Dec 2009
UTBLK	Asphalt	Jan 2009 - Dec 2009
UTDOG	Asphalt	Jan 2009 - Dec 2009
UTHEB	Asphalt	Jan 2009 - Dec 2009
UTICS	Asphalt	Jan 2009 - Dec 2009
UTLGP	Asphalt	Jan 2009 - Dec 2009
UTQRY	Asphalt	Jan 2009 - Dec 2009
UTR20	Asphalt	Jan 2009 - Dec 2009
UTSCI	Asphalt	Jan 2009 - Dec 2009
UTSLD	Asphalt	Jan 2009 - Dec 2009
UTSTV	Asphalt	Jan 2009 - Dec 2009
UTCKH	Both	Not Used
CCS	Concrete	Jan 2007 - Dec 2007
CEN	Concrete	Jan 2009 - Dec 2009
UT7	Concrete	Jan 2009 - Dec 2009
UT11	Concrete	Jan 2004 - Dec 2004
UT12	Concrete	Jan 2007 - Dec 2007
UT21	Concrete	Jan 2009 - Dec 2009
UT29	Concrete	Oct 2008 - Aug 2009
UTHEB	Concrete	Jan 2009 - Dec 2009
UTMFS	Concrete	Jan 2009 - Dec 2009

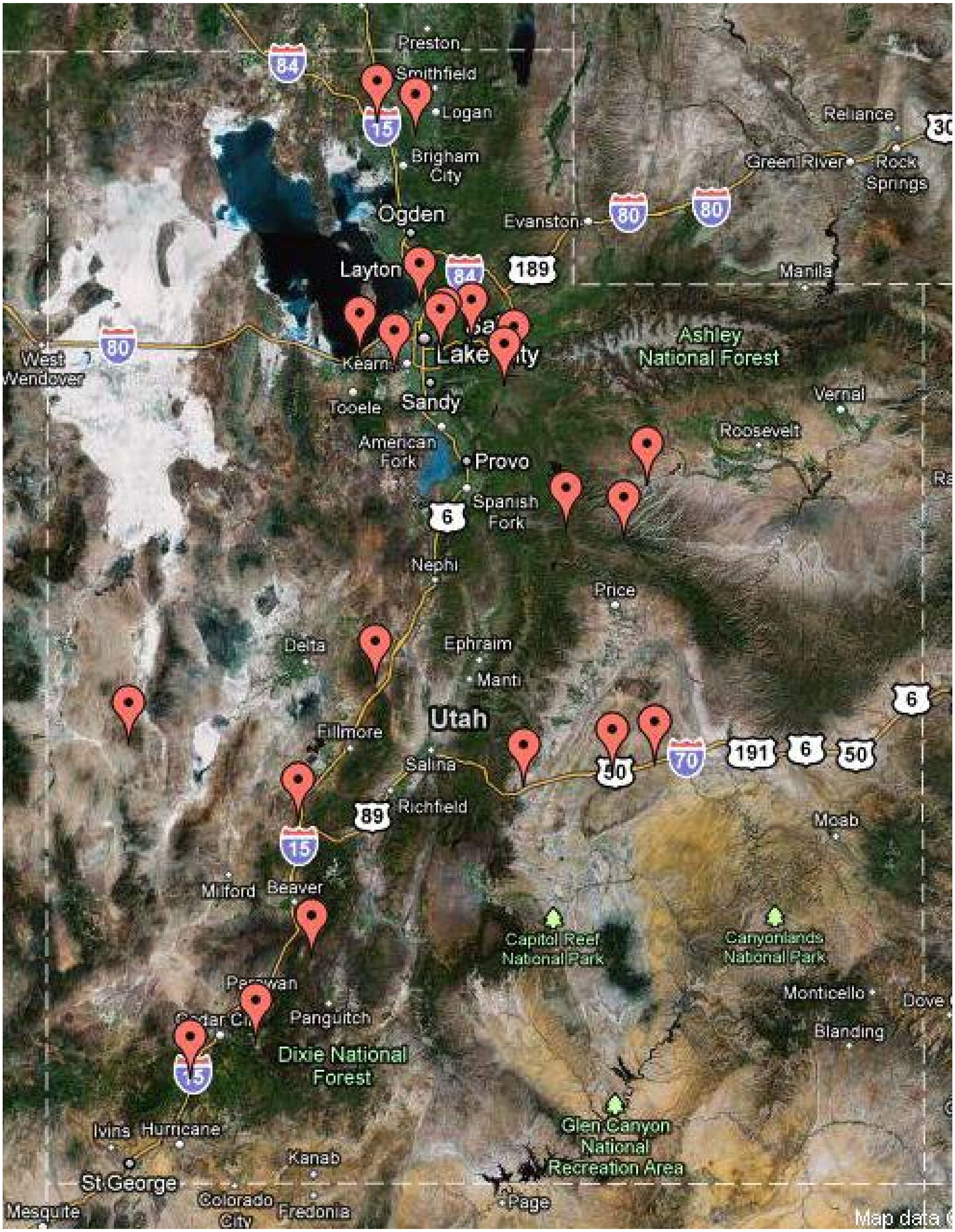
Preston
84
Smithfield
Logan
15
Brigham City
Ogden
Reliance
Green River
Rock Springs
Evanston
80
80
Manila
Layton
84
189
Ashley National Forest
West Wendover
80
Kearn
Lake City
Tooele
Sandy
Vernal
Roosevelt
American Fork
Provo
Spanish Fork
6
Nephi
Price
Delta
Ephraim
Manti
Utah
6
Fillmore
Salina
50
70
191
6
50
89
Richfield
Moab
15
Milford
Beaver
Capitol Reef National Park
Canyonlands National Park
Monticello
Blanding
Panguitch
Dixie National Forest
15
Glen Canyon National Recreation Area
Ivins
Hurricane
Kanab
St George
Mesquite
Colorado City
Fredonia
Page
Map data

Figure 3.3 RWIS stations on asphalt roads (*28*).

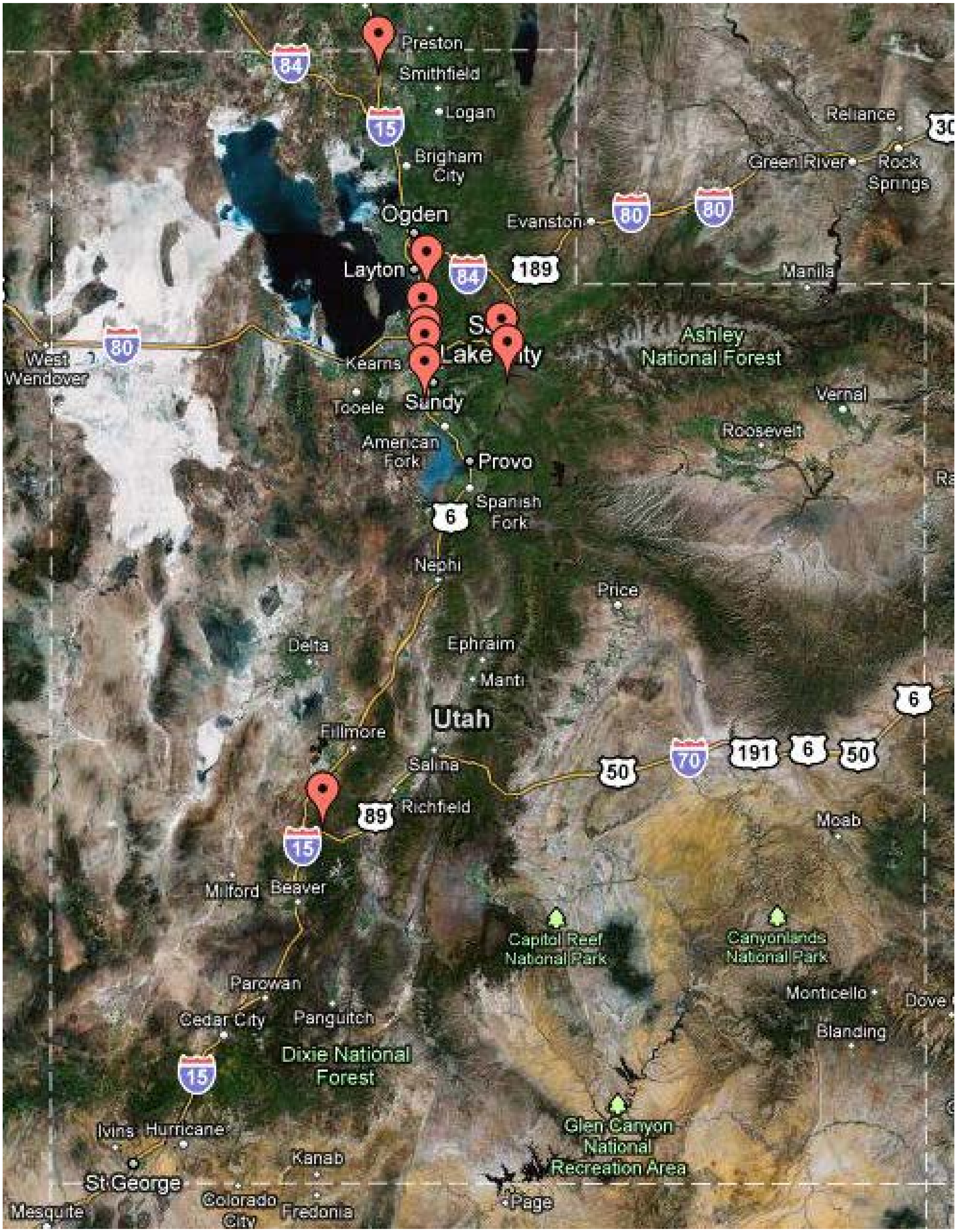
Preston
Smithfield
84
Logan
15
Reliance
30
Brigham City
Green River
Rock Springs
Ogden
Evanston
80
80
Layton
84
189
Manila
Lake
Ashley National Forest
West Wendover
80
Kearns
Tooele
Sandy
Vernal
Roosevelt
American Fork
Provo
Spanish Fork
6
Nephi
Price
Ephraim
Manti
Delta
6
Utah
Fillmore
Salina
50
70
191
6
50
Richfield
89
Moab
15
Milford
Beaver
Capitol Reef National Park
Canyonlands National Park
Parowan
Monticello
Cedar City
Panguitch
Blanding
Dixie National Forest
15
Glen Canyon National Recreation Area
Ivins
Hurricane
Kanab
St George
Colorado City
Fredonia
Page
Mesquite

Figure 3.4 RWIS stations on concrete roads (*28*).

3.3 Data Management

Because of the large amounts of data that were analyzed in this research, a macro was developed to automatically loop through all of the data and assimilate the individual RWIS files into a single database. The macro then removed any incorrect or unnecessary data, divided the data into time periods, and calculated the number of monthly subsurface freeze-thaw cycles. The following sections detail the algorithms that were used in deciding which data values were incorrect, which time stamps belonged in each time period, and how many freeze-thaw cycles occurred in each month.

3.3.1 Removal of Incorrect or Unnecessary Data

After all the necessary data were downloaded, and after the macro had assimilated the individual files into a single file, the combined data set had over 1.5 million rows of data. Unfortunately, not all of the data were usable. ESSs often give erroneous data because of sensor malfunctions (*29*), so problematic rows, as defined by the following criteria, were deleted from the data set:

- Missing air temperature
- Missing road temperature
- Air temperature less than −34°C (−30°F)
- Road temperature less than −34°C (−30°F)
- Air temperature or road temperature that stayed constant or nearly constant for at least 12 hours
- Air temperature or road temperature that differed from the previous and following temperatures by more than four times the difference between the previous two temperatures and the following two temperatures (spikes in the data)
- Entries from 16:00 on the last day of the month until 18:00 on the first day of the next month for stations UT28 and UT29, which systematically recorded linearly varying temperatures during these times

The cutoff point of −34°C (−30°F) was chosen due to a natural gap in the data between −26°C (−15°F), a reasonable low temperature for Utah weather, and −34°C (−30°F), an unreasonably low temperature. All temperatures below −34°C (−30°F) were obviously caused by errors in the pavement sensors. Additionally, time stamps that did not fall on the hour were deleted to reduce the sheer volume of data. This process of data reduction resulted in a much more manageable data set of about 220,000 entries.

One other complication was that a few of the stations had two road temperatures (labeled TRD1 and TRD2) for the same time stamp. Station UT11 had one road puck for each direction of travel, and, since both road temperatures were nearly identical, the TRD2 data were discarded, and the TRD1 data were retained, even when some values were missing from TRD1 that were available in TRD2. Station UTQRY had one puck for TRD1 and one tower-mounted non-intrusive pavement sensor for TRD2, so the TRD2 data were discarded, and the TRD1 data were retained. Because station UTHEB is located at the junction of a concrete pavement and an asphalt pavement, with one pavement sensor embedded in the asphalt pavement and the other pavement sensor embedded in the concrete pavement, both TRD1 and TRD2 data were used. Consequently, station UTHEB was treated as two different stations, as shown in Table 3.2, in which the asphalt and the concrete pavements had identical atmospheric data but differing pavement data.

3.3.2 Division of Data into Time Periods

Because the times corresponding to maximum temperatures, minimum temperatures, and inflection points change based on season, the data could not be grouped by fixed times. Instead, the data were divided into time periods that were based on sunrise and sunset times. Initially, the data set was divided into two groups: *light* and *dark*, where *light* starts one hour after sunrise and ends two hours after sunset, and *dark* starts two hours after sunset and ends one hour after sunrise. These cutoff points were chosen because they corresponded to the points at which the pavements started heating up and stopped cooling down, as described in Section 2.3 of this report.

Light and *dark* were then further divided into three periods each. *Light* was divided into the categories of *late morning*, *early afternoon*, and *late afternoon*, while *dark* was divided into the categories of *evening*, *night*, and *early morning*. Table 3.3 gives a description of each of these time periods.

Because of the change of seasons, *evening*, for example, does not start at the same hour for all months of the year. Average sunrise and sunset times were found by using the sunrise and sunset times from the 15th day of each month (*30*). Further, all stations were assumed to have the same sunrise and sunset times as Salt Lake City. Table 3.4 shows how the 24-hour day was divided into the six time periods for each month of the year.

To verify the assumption that all stations have the same sunrise and sunset time in a given month, six stations were chosen from extreme latitude and longitude combinations, and the pavement temperatures were plotted for the 15th of each month. Figure 3.5 shows the road surface temperature plotted for each hour of January 15th.

Similar plots for each month of the year are shown in the appendix, illustrating that the six times of day accurately divide the data into representative time periods. *Late morning* captures the portion of the day when the pavement is warming up; e*arly afternoon* captures the hottest part of the day; and *late afternoon*, *evening*, *night*, and *early morning* capture the pavement cooling down. These observations hold true for all months and all stations, on average.

Table 3.3 Description of Time Periods

Time Period	**Description**
Late Morning	First third of *light*
Early Afternoon	Middle third of *light*
Late Afternoon	Last third of *light*
Evening	First third of *dark*
Night	Middle third of *dark*
Early Morning	Last third of *dark*

Table 3.4 Time Periods for Late Morning, Early Afternoon, Evening, Night, and Early Morning Based on Month

Month	Late Morning	Early Afternoon	Late Afternoon	Evening	Night	Early Morning
January	9:00-12:00	13:00-15:00	16:00-19:00	20:00-23:00	0:00-4:00	5:00-8:00
February	9:00-12:00	13:00-16:00	17:00-20:00	21:00-23:00	0:00-4:00	5:00-8:00
March	8:00-11:00	12:00-16:00	17:00-20:00	21:00-0:00	1:00-3:00	4:00-7:00
April	7:00-11:00	12:00-16:00	17:00-21:00	22:00-0:00	1:00-3:00	4:00-6:00
May	7:00-11:00	12:00-16:00	17:00-21:00	22:00-0:00	1:00-3:00	4:00-6:00
June	6:00-11:00	12:00-16:00	17:00-22:00	23:00-0:00	1:00-3:00	4:00-5:00
July	7:00-11:00	12:00-16:00	17:00-21:00	22:00-0:00	1:00-3:00	4:00-6:00
August	7:00-11:00	12:00-16:00	17:00-21:00	22:00-0:00	1:00-3:00	4:00-6:00
September	7:00-11:00	12:00-16:00	17:00-20:00	21:00-0:00	1:00-3:00	4:00-6:00
October	8:00-11:00	12:00-15:00	16:00-19:00	20:00-23:00	0:00-3:00	4:00-7:00
November	9:00-11:00	12:00-15:00	16:00-19:00	20:00-23:00	0:00-3:00	4:00-8:00
December	9:00-12:00	13:00-15:00	16:00-19:00	20:00-23:00	0:00-4:00	5:00-8:00

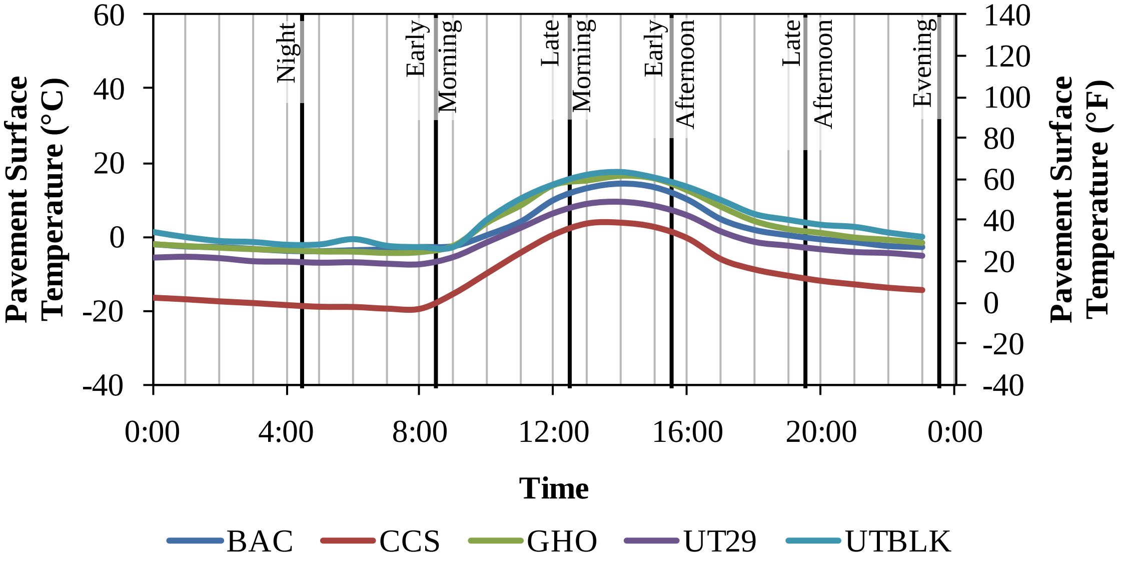

Figure 3.5 Typical pavement surface temperatures for each time period.

3.3.3 Calculation of Monthly Freeze-Thaw Cycles

Because adjacent freezing events, sequential in time, must be separated by a thawing event, counting the number of freezes is identical to counting the number of thaws. If data from every hour and every station were available, counting the number of freeze-thaw cycles in a year would be very easy. However, because of missing or erroneous data, a more complicated algorithm had to be developed for this research. To determine the number of air or subsurface freeze-thaw cycles in a month, the number of measured freeze-thaw cycles was scaled up by the ratio of total days in the month to total days with data. Some of the stations, however, had only a few days of good data in a month. Because extrapolating only a few days of data to the whole month may yield inaccurate estimates, the data for a given month at a given station was excluded from the analysis if the data set had fewer than 7 days of data (20 percent) for that month at that station.

A day was considered to have sufficient data if at least one of the following two conditions were met: 1) at least one hour was below freezing and at least one hour was above freezing, or 2) at least one record from 4:00 to 8:00 was available, and at least one record from 12:00 to 16:00 was available. A day was considered to have experienced a freeze-thaw cycle if both of the following conditions were met: 1) the day had sufficient data, and 2) the maximum temperature was above freezing and the minimum temperature was below freezing.

This logic is based on several assumptions, which may or may not be correct in every situation:

- Each day in the month is representative of the month
- No day has more than one freeze-thaw cycle
- The hours from 4:00 to 8:00 contain the coldest temperatures of the day
- The hours from 12:00 to 16:00 contain the hottest temperatures of the day

Even though these assumptions may not apply in every situation, they describe typical days, and they were helpful in extrapolating needed values from the available data so that the statistical analysis described in Section 3.4.2 could be performed. In the event of a storm, some days may have mid-day air temperatures that dip below freezing. Such days would then experience two freeze-thaw cycles with regards to air temperature. However, for the subgrade 45 cm (18 in.) under the pavement, the ranges in time in which maximum and minimum temperatures occur are so close to each other that, with typical thermal gradients, the pavement could not cool and heat fast enough within the given time period to cause a second subsurface freeze-thaw cycle on those days. Thus, for a given day, if the coldest temperature between 4:00 and 8:00 is above freezing and the hottest temperature between 12:00 and 16:00 is also above freezing, then any missing data from other hours of the day would likely not be below freezing. Therefore, the data are sufficient to assume that such a day experienced no freeze-thaw cycles, even if some of the data are missing.

3.4 Statistical Analyses

In alignment with the research objectives, two statistical analyses were conducted to determine the differences in pavement surface temperature between asphalt and concrete pavements and to determine the number of subsurface freeze-thaw cycles under the same pavements. The following sections detail the procedures used to perform the statistical analyses.

3.4.1 Pavement Surface Temperatures

The first objective of this research was to compare the surface temperatures of asphalt and concrete pavements to determine which pavement type requires more winter maintenance. Because the ESSs are scattered across Utah, the surface temperatures cannot be compared without first accounting for climatic differences among the separate locations. Therefore, a multiple linear regression model was developed to predict pavement surface temperature based on elevation, latitude, longitude, air temperature, 45 cm (18 in.) underground temperature, time period, and pavement type. Wind direction and wind speed were not used because these values were not recorded for one third of the concrete stations. Relative humidity was not used because the literature provides no theoretical or logical reasons for relative humidity to influence pavement temperature. Solar radiation was not used because it was not available for any of the concrete roads; instead, latitude was used as a surrogate measure of solar radiation. Precipitation was not used because some of the ESSs provided *yes* or *no*, some of the ESSs provided the rate of precipitation, and most of the ESSs provided no precipitation data at all.

3.4.2 Subsurface Freeze-Thaw Cycles

The second objective of this research was to compare the temperatures 45 cm (18 in.) under asphalt and concrete pavements to determine the pavement type below which more freeze-thaw cycles of the underlying soil occur. The depth of 45 cm (18 in.) was chosen because the subsurface temperature probes installed at ESSs in Utah measure temperatures at this depth. A common statistical approach used to determine if a single parameter of interest affects the dependent variable is to create the best statistical model possible excluding that parameter of interest and then add the parameter of interest to the model (*31*). Consistent with this approach, pavement type, as the parameter of interest, was initially excluded, and the best model predicting subsurface freeze-thaw cycles was determined. After the best model that excluded pavement type was found, pavement type was added to the model to determine the effect of pavement type on subsurface freeze-thaw cycles.

The initial independent variables used to predict the number of subsurface freeze-thaw cycles were month, elevation, latitude, and number of air freeze-thaw cycles. Month was treated as a categorical variable, and the rest were treated as continuous variables. The method of backward selection was used to determine which input variables best helped predict the number of subsurface freeze-thaw cycles. To determine if an independent variable should be included in the final model, a nominal *p*-value of 0.10 was used (*32*). A *p*-value of 0.10 was used instead of a more stringent *p*-value of 0.05 because the latter led to a model with only one independent variable.

3.5 Finite-Difference Modeling

This section details how a finite-difference model was created to predict surface temperatures for asphalt and concrete pavements based on albedo, specific heat, and thermal conductivity. Formulas were derived from basic heat flow theory. Since volume is the product of area and thickness and since energy is the product of radiosity, area, and time, Equation 2.1 can be rearranged to form Equation 3.1:

$$\Delta T = \frac{R \cdot t}{c \cdot d} \tag{3.1}$$

where: ΔT = average increase in temperature (°C)

R = radiosity ($\mathrm{W/m^2}$)

t = time (sec)

c = specific heat ($\mathrm{J\ m^{-3}\ °C^{-1}}$)

d = thickness of material (m)

Equation 3.1 applies when the temperature increases uniformly for the whole volume of pavement. However, since the pavement surface heats up first, producing a thermal gradient that causes the energy to move down deeper into the pavement, the equation cannot be applied directly. Nonetheless, Equation 3.1 is valid for small values of d and t, over which the temperature can be approximated as constant.

Radiosity is the amount of power per area (heat) that is transferred from one layer of pavement to the next. With this substitution, Equation 2.2 can be simplified to produce Equation 3.2:

$$R = k\frac{\Delta T}{\Delta h} \tag{3.2}$$

where: R = radiosity (W/m^2)

k = thermal conductivity (W m^{-1} °C^{-1})

ΔT = difference in temperature across Δh (°C)

Δh = thickness of layer (m)

Equation 3.2 shows that the radiosity transmitted across a distance Δh is proportional to the thermal conductivity of the material and to the difference in temperature across Δh. Thus, a higher thermal conductivity and a higher temperature gradient both allow for more heat to be transferred.

To supplement the statistical analysis described in Section 3.4.1, a simple finite-difference analysis was conducted using Equations 3.1 and 3.2. Figure 3.6 shows a schematic of the finite-difference model, and Table 3.5 shows the material properties used in the model. Only heat flow was calculated in the model; moisture content, salinity, and other parameters were not calculated. A model thickness of 1 m (3 ft) was used, and the simulated layer was assumed to be homogenous due to a lack of pavement thickness data for the actual pavements studied in this research. This assumption is acceptable for the purposes of this modeling because material properties close to the surface are much more influential on surface temperature than material properties several centimeters under the surface. That is, the subsurface material properties do not affect the results of the simulation significantly. The pavement was divided into 0.01-m-thick layers (0.03 ft), and temperatures were calculated every 30 seconds for two different

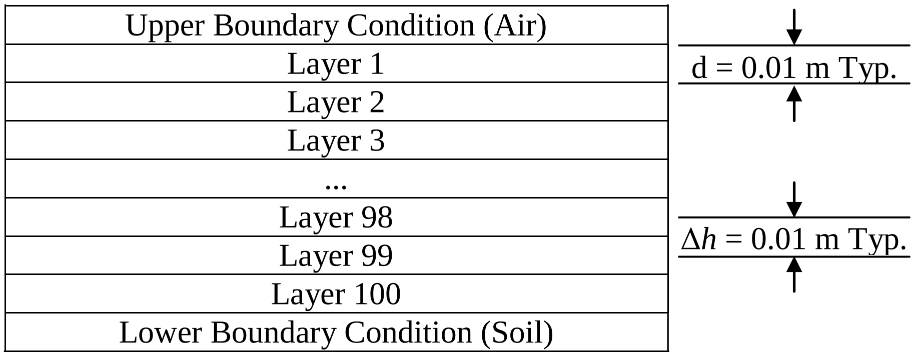

Figure 3.6 Schematic of finite-difference model.

Table 3.5 Material Properties Used in Finite-Difference Model

Material Property	Asphalt	Concrete
Albedo	0.12	0.33
Specific Heat (J m^{-3} $°C^{-1}$)	1.42	2.07
Thermal Conductivity (W m^{-1} $°C^{-1}$)	0.74	1.69

simulations. For both simulations, the pavement temperature was set to 0°C (32°F) for all layers at the beginning of the simulation, and the lower boundary condition was set to 0°C (32°F) for the duration of the simulation. The upper boundary condition was set to 1°C (34°F) for the duration of both simulations. The only difference between the two simulations was that the first simulation had no incident solar radiation, while the second simulation had 100 W/m^2 of incident solar radiation.

In general terms, energy from solar radiation and from warm air enters the surface of the pavement, causing the temperature in Layer 1 of the pavement to increase slightly according to Equation 3.1. This increased surface temperature causes a temperature gradient to form between Layer 1 and Layer 2. The heat transferred from Layer 1 to Layer 2 can then be calculated using Equation 3.2. This transfer of energy causes an increase in the temperature of Layer 2 and a decrease in the temperature of Layer 1. While the heat is being transferred from Layer 1 to Layer 2, Layer 1 is simultaneously being heated by solar radiation and warm air. Thus, with small time increments and small layer thicknesses, temperature profiles can be established (*6, 33*).

3.6 Summary

Data from two sources had to be combined into a single database for this research. Climatological data were acquired from the MesoWest website, and pavement-type data were obtained from Google Maps. Twelve continuous months of data, primarily from the 2009 calendar year, were used for each station, and erroneous data were removed from the data set. Freeze-thaw cycles at a depth of 45 cm (18 in.) underground were counted, and the counts were scaled up based on the ratio of days in the month to days with data. To predict the pavement surface temperatures, a multiple linear regression was performed with input parameters of pavement type, time period, and air temperature. Similarly, a multiple linear regression was performed to predict the number of subsurface freeze-thaw cycles from the input parameters of month, latitude, elevation, and pavement type. These parameters were chosen using the method of backward selection. A finite-difference model was also created to model surface temperatures in asphalt and concrete pavements based on air temperature and incoming radiation.

4.0 RESULTS

4.1 Overview

This chapter presents the results of the statistical analyses and finite-difference modeling described in Chapter 3.

4.2 Statistical Analyses

The following two sections detail the results of the two statistical analyses that were performed to meet the two objectives of this research. The first statistical analysis compares the surface temperatures of asphalt and concrete pavements to determine which pavement type requires more winter maintenance. The second statistical analysis compares the number of freeze-thaw cycles that occur 45 cm (18 in.) under each pavement type to determine the pavement type below which more freeze-thaw cycles of the underlying soil occur.

4.2.1 Pavement Surface Temperatures

The results of the preliminary statistical analysis showed that pavement type was not a significant predictor of pavement temperature when all of the input parameters were used. Because pavement type, elevation, latitude, and longitude remained constant for all data points from a given station, these independent variables were highly correlated with each other. Consequently, the importance of pavement type could have been masked by these highly correlated variables.

Because including correlated variables could have led to an artificially good fit in this case, a linear regression analysis was performed using a reduced set of independent variables (pavement type, time period, and air temperature) to predict surface temperature. All two-way and three-way interactions were included, allowing for different slopes and intercepts for each combination of time period and pavement type, because the different thermal properties of asphalt and concrete suggest that the two materials will exhibit different pavement surface temperatures for different times of the day and different air temperatures. Slopes and intercepts were considered to be significantly different if their *p*-values were less than or equal to 0.05.

The resulting regression equations are given in Table 4.1. The variable $T_{pavement}$ represents the pavement surface temperature in °C, and the variable T_{air} represents the air temperature in °C. Time period descriptions were given previously in Table 3.1. The equations from Table 4.1 are shown graphically in Figures 4.1 through 4.6. Each chart shows the predicted pavement temperature for asphalt and concrete pavements during that specific time period.

Table 4.1 Regression Equations for Pavement Surface Temperatures

Time Period	**Asphalt**		**Concrete**	
	$T_{pavement}$, °C	**R^2**	**$T_{pavement}$, °C**	**R^2**
Late Morning	$1.145 \cdot T_{air} + 4.0$	0.8632	$1.103 \cdot T_{air} + 4.1$	0.9092
Early Afternoon	$1.325 \cdot T_{air} + 9.5$	0.8601	$1.257 \cdot T_{air} + 7.8$	0.8915
Late Afternoon	$1.230 \cdot T_{air} + 4.2$	0.9037	$1.174 \cdot T_{air} + 3.5$	0.9264
Evening	$1.060 \cdot T_{air} + 2.1$	0.9457	$1.029 \cdot T_{air} + 2.3$	0.9595
Night	$1{,}039 \cdot T_{air} + 1.5$	0.9318	$1.025 \cdot T_{air} + 2.0$	0.9560
Early Morning	$1.016 \cdot T_{air} + 1.3$	0.9237	$1.010 \cdot T_{air} + 1.8$	0.9530

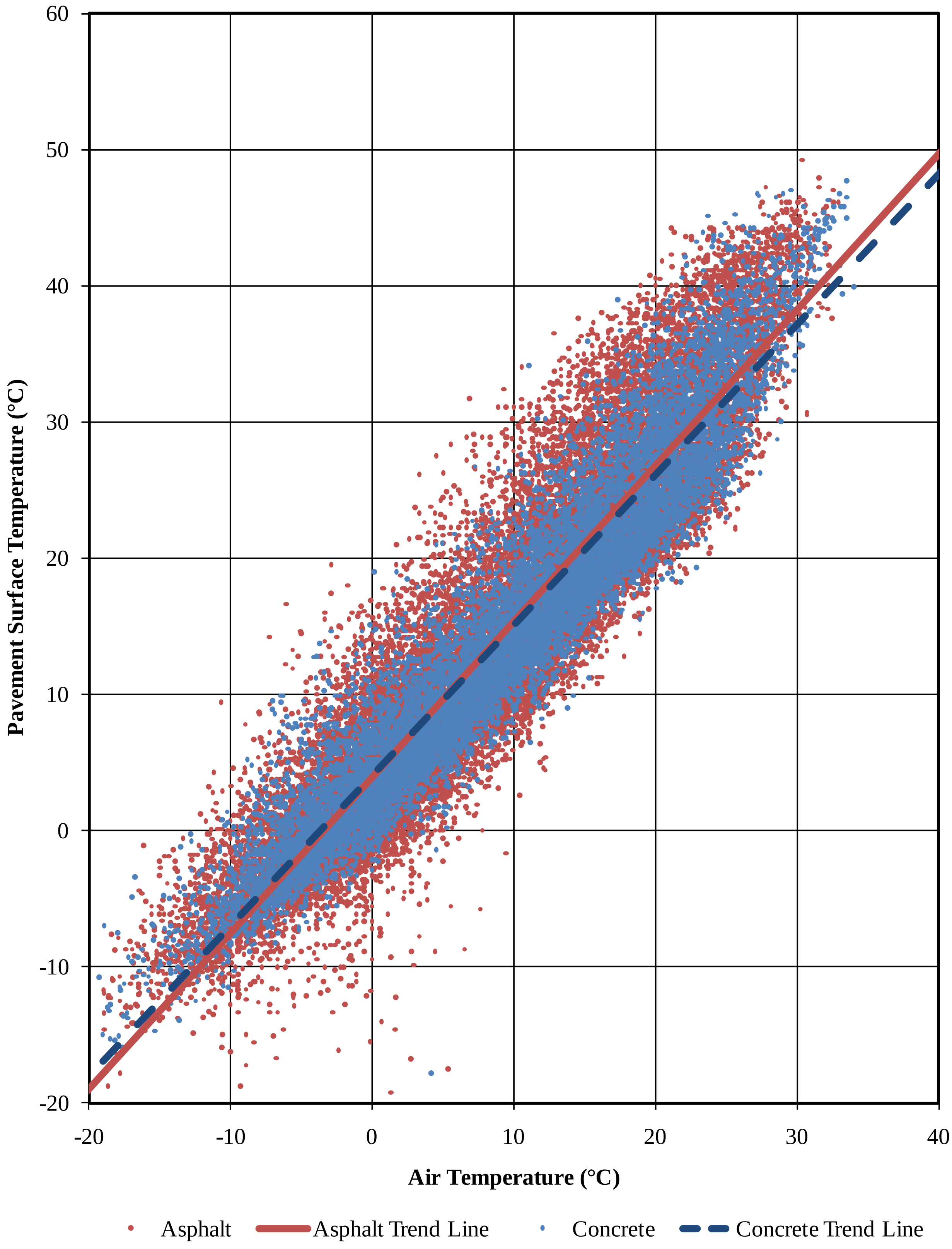

Figure 4.1 Predicted pavement surface temperatures for late morning.

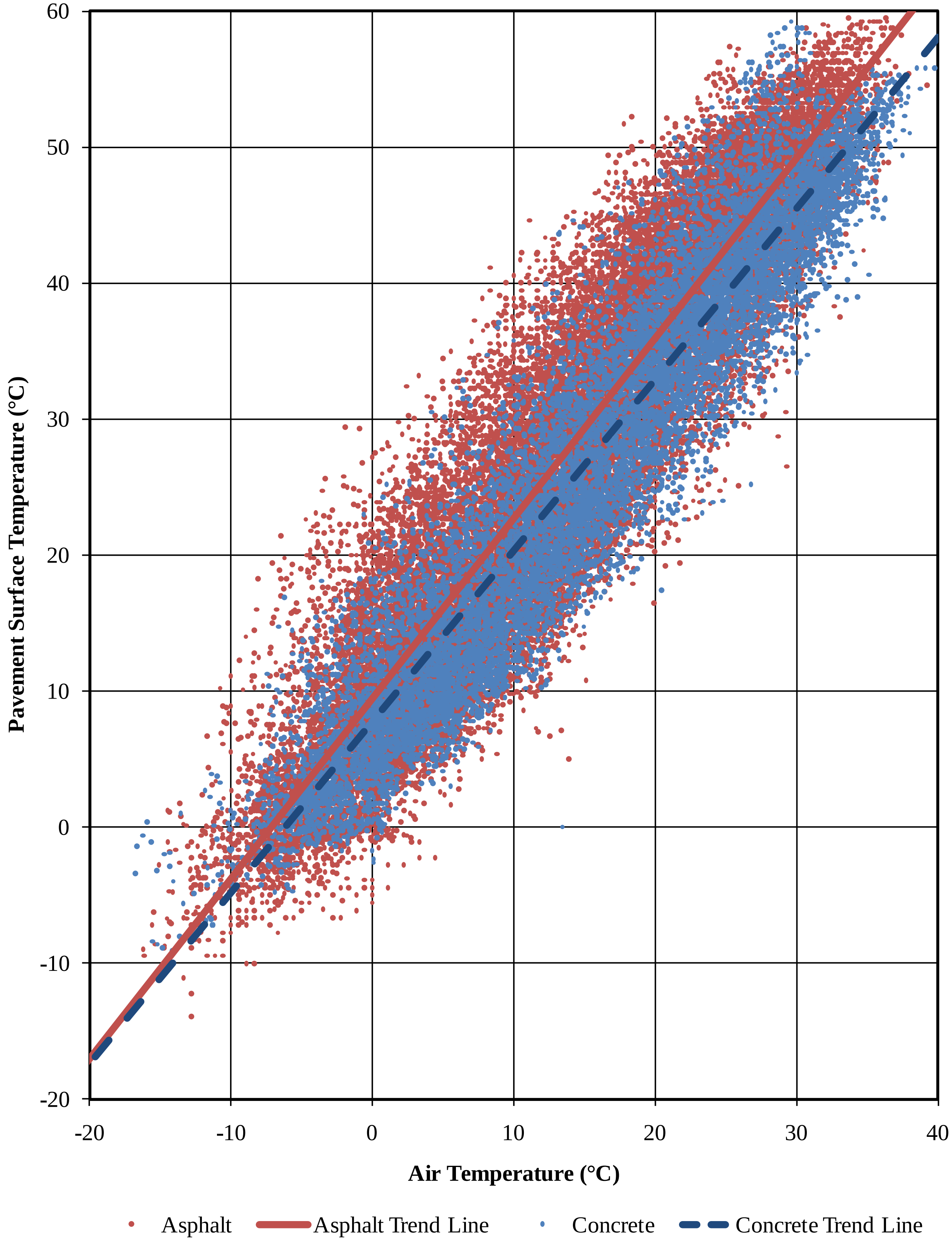

Figure 4.2 Predicted pavement surface temperatures for early afternoon.

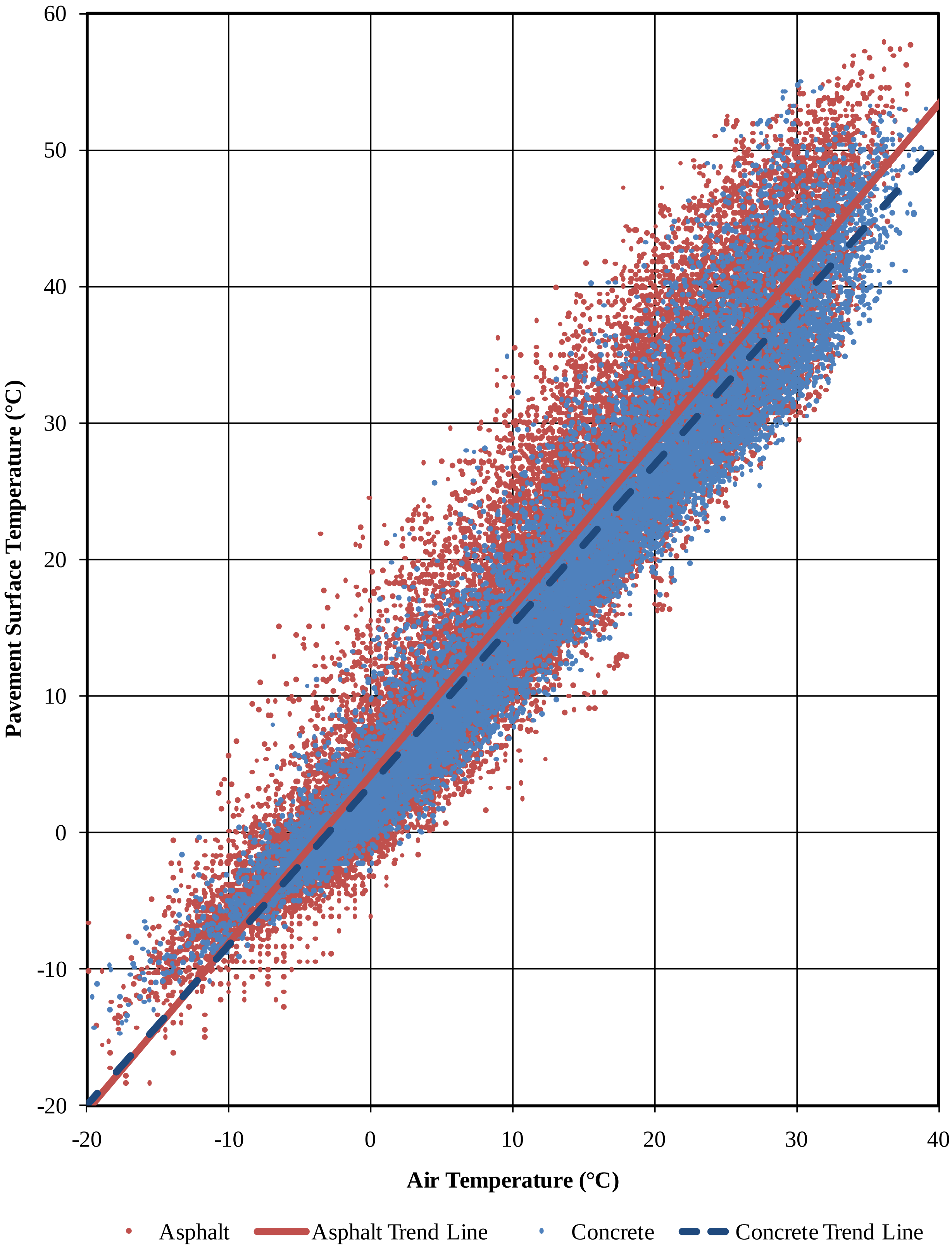

Figure 4.3 Predicted pavement surface temperatures for late afternoon.

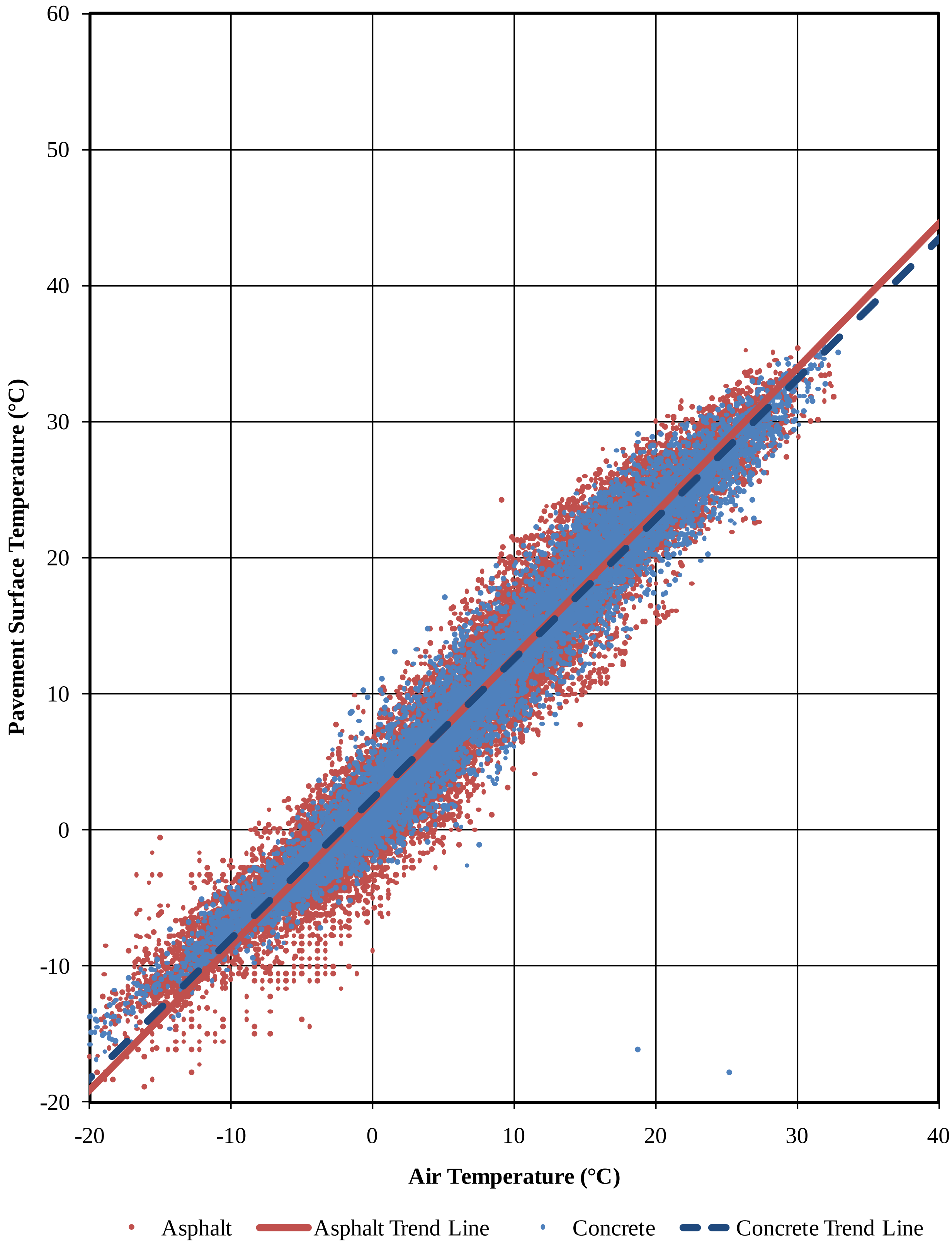

Figure 4.4 Predicted pavement surface temperatures for evening.

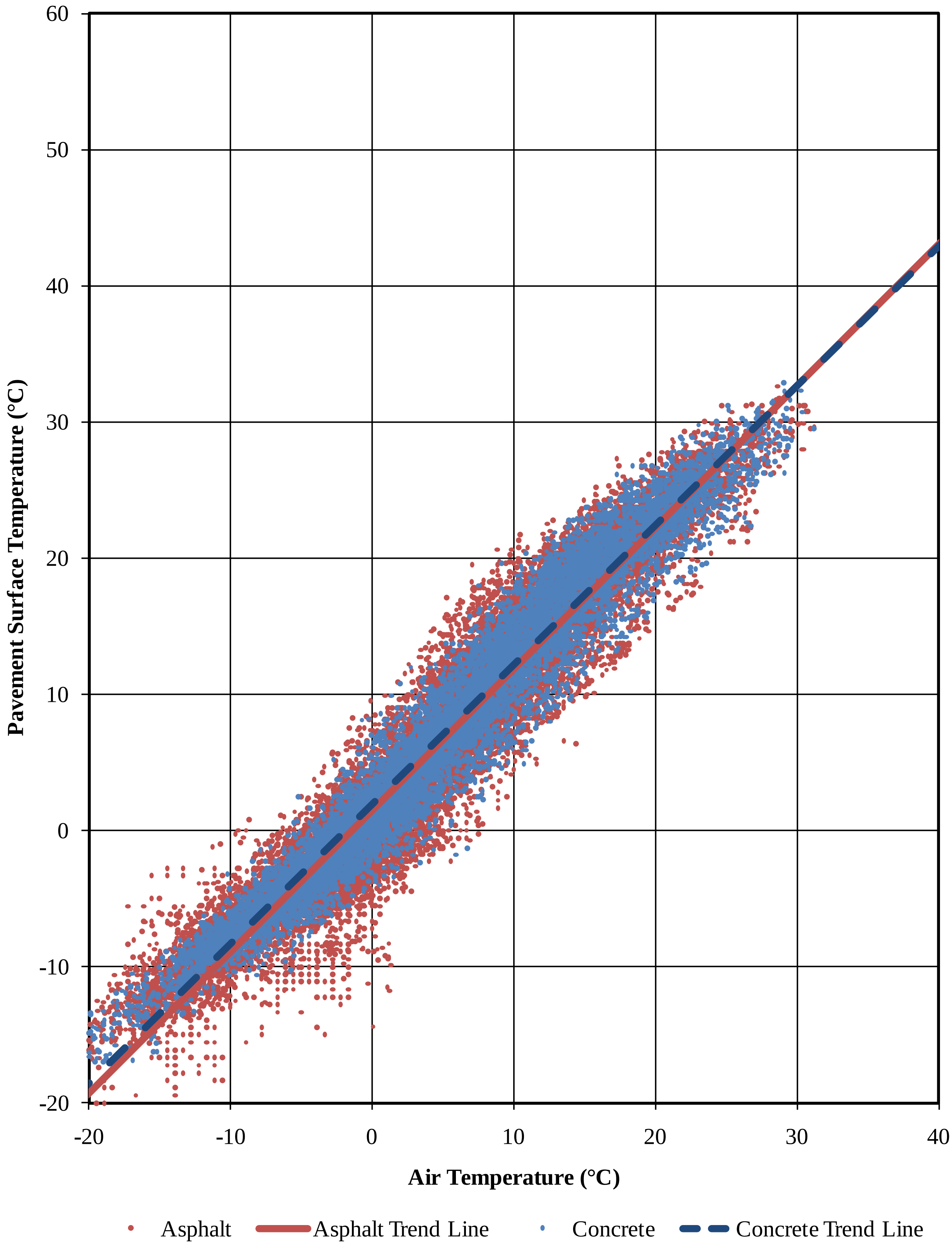

Figure 4.5 Predicted pavement surface temperatures for night.

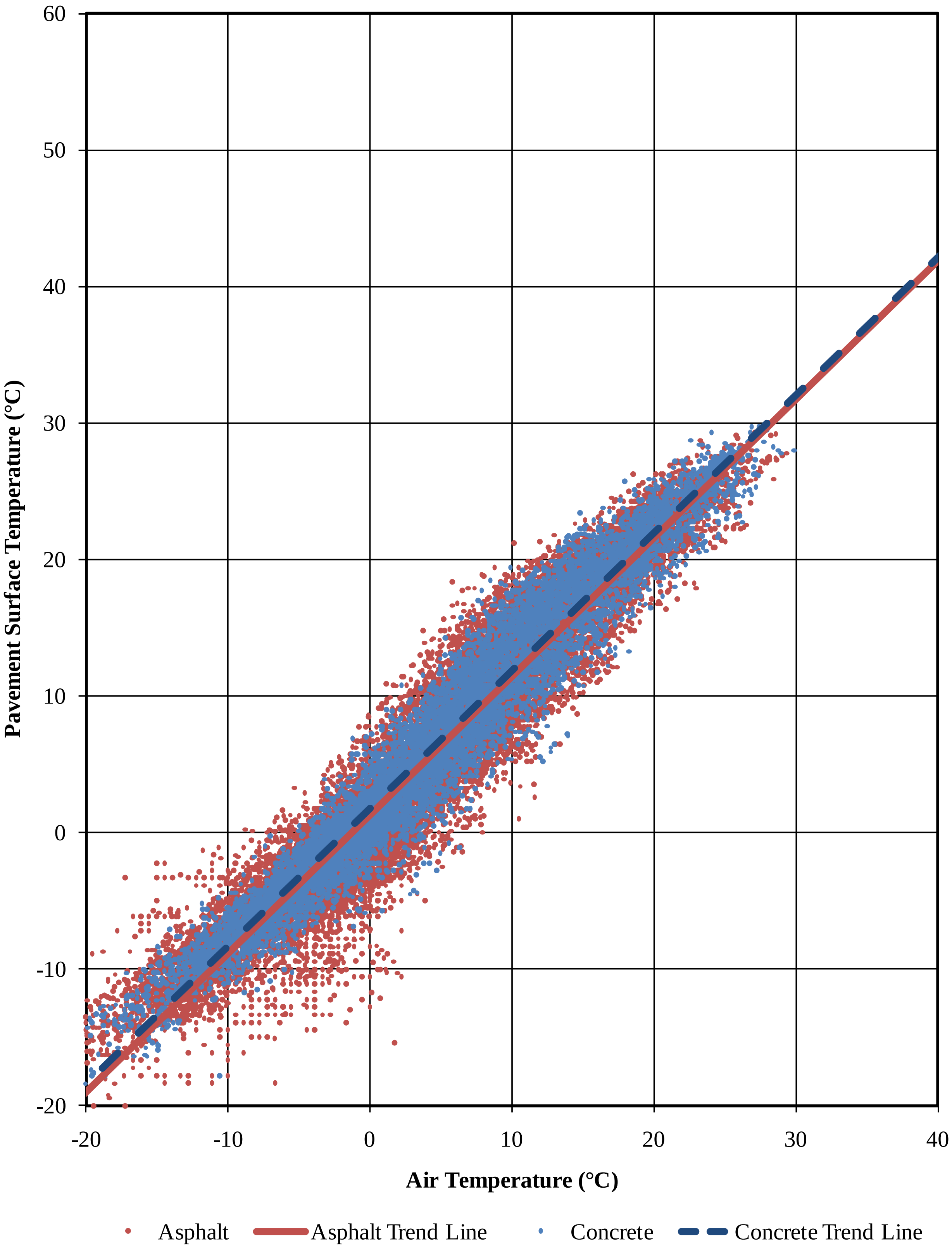

Figure 4.6 Predicted pavement surface temperatures for early morning.

Table 4.2 shows that, for each time period, the *y*-intercepts and slopes of the regression equations for asphalt and concrete pavement surface temperatures are, for the most part, statistically different from each other. With only two exceptions, the *p*-values are all less than 0.001. Only the *p*-values for the intercept and slope of the *late morning* and *early morning* time periods, respectively, have *p*-values greater than 0.05; a high *p*-value indicates, for example, that the *y*-intercept of 4.0, as shown in Table 4.1 for asphalt, is not statistically different from the *y*-intercept of 4.1 for concrete.

For ease in discussing these results, freezing will be assumed to occur at 0°C (32°F). Freezing of pore water inside the pavement does not usually occur at this temperature, but freezing generally does occur at 0°C (32°F) for rain, snow, and other surface water on top of the pavement, as long as it is in its pure form. With this definition of freezing, Figure 4.1, for example, shows that, for *late morning*, the asphalt pavement is expected to freeze when the air temperature reaches −3.5°C (25.8°F), and the concrete pavement is expected to freeze when the air temperature reaches −3.7°C (25.3°F). Therefore in *late morning*, while the air temperature is between −3.5°C (25.8°F) and −3.7°C (25.3°F), the asphalt pavement is expected to freeze, and the concrete pavement is expected to remain unfrozen. Similarly, Figure 4.2 shows that the asphalt pavement in *early afternoon* is expected to freeze when the air temperature reaches −7.2°C (19.1°F) compared to −6.2°C (20.9°F) for concrete pavement. Figures 4.3 to 4.6 can be interpreted in a similar manner.

Table 4.2 Results of Statistical Analyses for Prediction of Pavement Surface Temperatures

Time Period	Intercepts *p*-value	Slopes *p*-value
Late Morning	0.0586	<0.001
Early Afternoon	<0.001	<0.001
Late Afternoon	<0.001	<0.001
Evening	<0.001	<0.001
Night	<0.001	<0.001
Early Morning	<0.001	0.0696

Table 4.3 shows the predicted air temperatures for which the pavement temperatures are 0°C (32°F). The expected differences in air temperatures are also shown. The variable ΔT_{air} represents the air temperature when the asphalt pavement is 0°C (32°F) minus the air temperature when the concrete pavement is 0°C (32°F).

The difference in air temperatures corresponding to freezing pavement surface temperatures shows that snow and ice are less likely to accumulate on concrete pavements for all time periods except *early afternoon* and *late afternoon*. An explanation for why asphalt is warmer in early and late afternoon and colder during all other times of the day requires consideration of the albedo of asphalt and concrete. Asphalt absorbs more solar energy than concrete because asphalt has a lower albedo. Consequently, during hours with significant solar radiation, asphalt should logically have higher pavement surface temperatures. The larger specific heat and larger thermal conductivity of concrete tend to cancel each other out, resulting in surface temperature differences dominated largely by albedo.

The results of the statistical analysis performed using all available terms indicate that pavement type is not a significant predictor of surface temperature, but the results of the statistical analysis performed using a reduced number of terms indicate that pavement type is a significant predictor of surface temperature. Although the second analysis shows a statistical difference between surface temperatures for asphalt and concrete pavements, it does not reveal a practical difference. For one pavement type to require

Table 4.3 Air Temperatures Corresponding to Freezing Pavement Surface Temperatures

Time Period	**T_{air} at $T_{pavement}$ = 0°C (32°F)**		**ΔT_{air} °C (°F)**	**Requires Less Winter Maintenance**
	Asphalt	**Concrete**		
Late Morning	−3.5 (25.8)	−3.7 (25.3)	0.2 (0.4)	Concrete
Early Afternoon	−7.2 (19.1)	−6.2 (20.9)	−1.0 (−1.8)	Asphalt
Late Afternoon	−3.4 (25.9)	−3.0 (26.6)	−0.4 (−0.7)	Asphalt
Evening	−2.0 (28.4)	−2.2 (28.0)	0.3 (0.4)	Concrete
Night	−1.4 (29.3)	−2.0 (28.5)	0.5 (0.8)	Concrete
Early Morning	−1.3 (29.6)	−1.8 (28.8)	0.5 (0.8)	Concrete
Average	−3.1 (26.4)	−3.1 (26.4)	0.0 (0.0)	Neither

less winter maintenance, it needs to have surface temperatures several degrees higher than the other pavement type, and since no road has one pavement type during the day and a different pavement type at night, the temperature needs to be consistently higher for all times of the day. The average ΔT_{air} of all the time periods is 0.0°C (0.0°F), showing that, although asphalt is better in the afternoon, and concrete is better for other times of the day, neither pavement type is better, on average. The possibility remains that one pavement type may require more winter maintenance because of rutting, surface texture, or other factors not considered in this analysis. However, from the standpoint of surface temperatures, asphalt and concrete are equally likely to collect snow or ice on their surfaces, and both pavements are expected to require equal amounts of winter maintenance, on average.

4.2.2 Subsurface Freeze-Thaw Cycles

Figure 4.7 shows the observed number of subsurface freeze-thaw cycles versus month for a depth of 45 cm (18 in.). The data were jittered (randomly perturbed) within each month category to reveal overlapping data points in the figure. Figure 4.8 shows the number of monthly subsurface freeze-thaw cycles versus elevation, Figure 4.9 shows the number of monthly subsurface freeze-thaw cycles versus latitude, and Figure 4.10 shows the number of monthly subsurface freeze-thaw cycles versus longitude. These figures show that an obvious correlation exists between freeze-thaw cycles and month but that no obvious correlations exist between monthly freeze-thaw cycles and elevation, latitude, or longitude.

For the initial statistical modeling of these data, the dependent variable was the number of subsurface freeze-thaw cycles, and the independent variables were month, elevation, latitude, and number of air freeze-thaw cycles. This analysis showed that the number of air freeze-thaw cycles (*p*-value of 0.9241) was not a significant predictor of subsurface freeze-thaw cycles after accounting for all other variables. Subsequently, the number of air freeze-thaw cycles was excluded from consideration, and another model

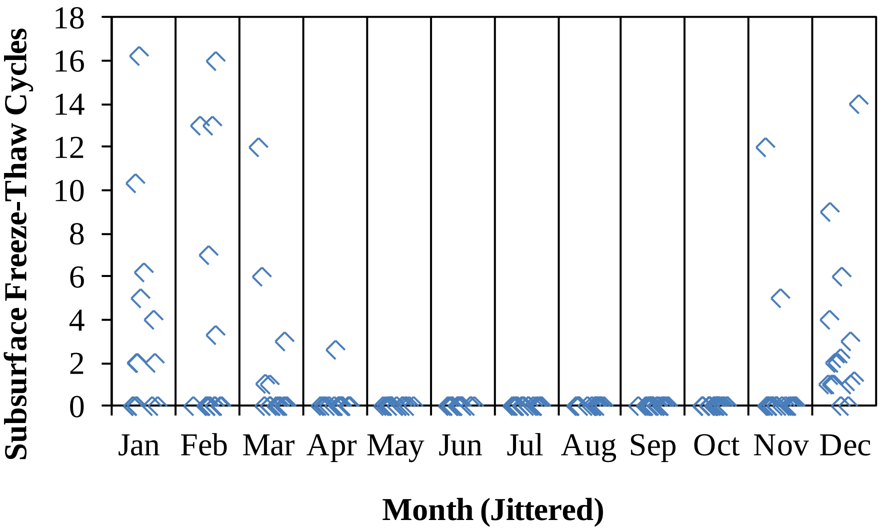

Figure 4.7 Number of subsurface freeze-thaw cycles versus month.

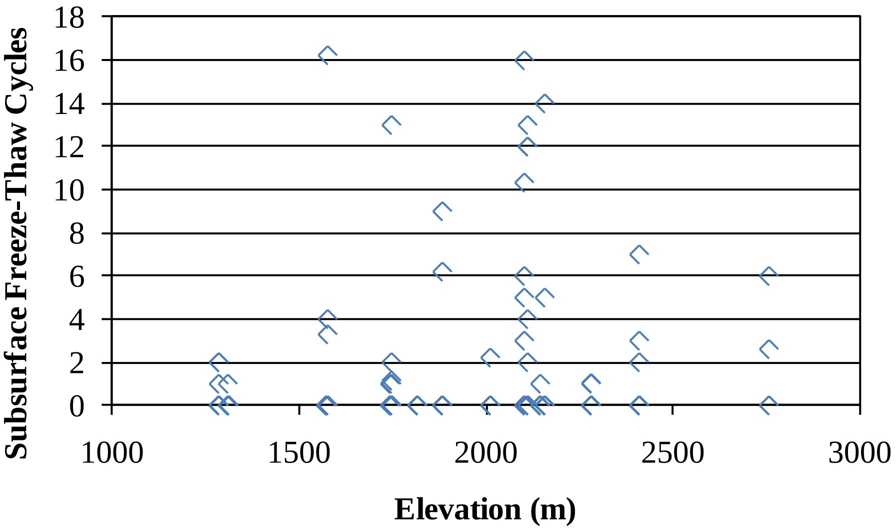

Figure 4.8 Number of monthly subsurface freeze-thaw cycles versus elevation.

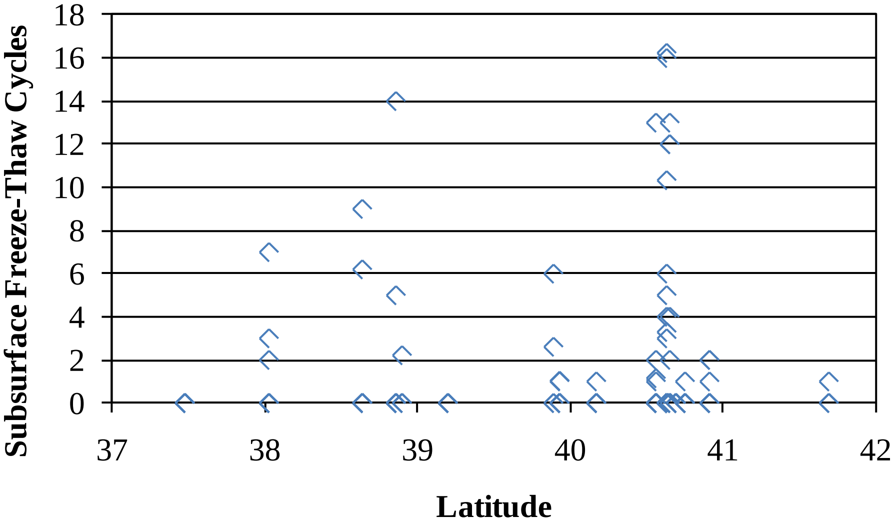

Figure 4.9 Number of monthly subsurface freeze-thaw cycles versus latitude.

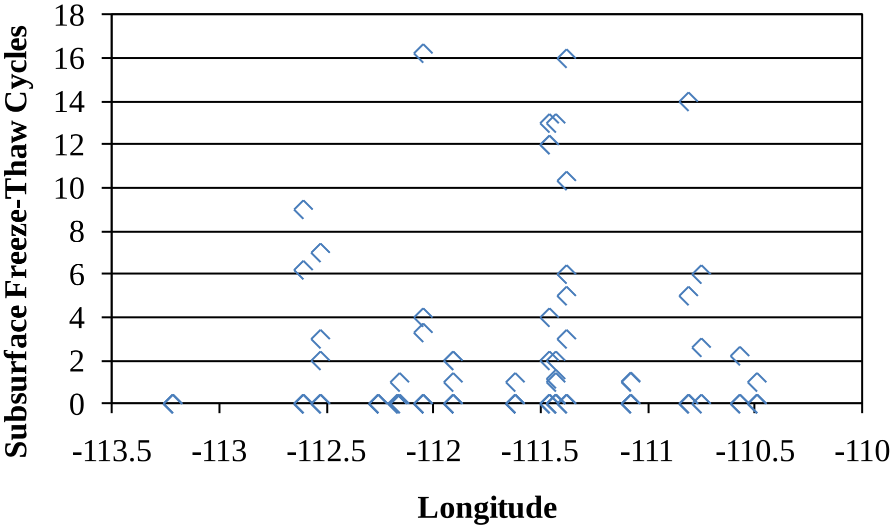

Figure 4.10 Number of monthly subsurface freeze-thaw cycles versus longitude.

was prepared. All terms in the second model had *p*-values less than or equal to 0.10 and were therefore retained.

The final multiple regression analysis was then performed with the input parameters of month, elevation, and latitude together with the addition of pavement type. The results of the statistical analysis are shown in Table 4.4. Hyphens are used to show when either *Month* or *Pavement* was not used to compute the *Estimate* or when calculation of a *p*-value was not applicable. The output shows that most terms in the model are statistically suggestive (*p*-values less than 0.10). More specifically, elevation, with a *p*-value of 0.0801, is statistically suggestive, while latitude, with a *p*-value of 0.2223, is not statistically suggestive. A *p*-value was not computed for the month of December or for the pavement type of concrete because these parameters were used in the analyses as references to which the other months and the pavement type of asphalt were compared. The numbers of subsurface freeze-thaw cycles in January, February, and

Table 4.4 Results of Statistical Analyses for Predicting Subsurface Freeze-Thaw Cycles

Parameter	Month/Pavement	Estimate	*p*-value
Intercept	-	−7.91873	0.3748
Elevation	-	0.000324	0.0801
Latitude	-	0.253717	0.2223
Month	January	0.309161	0.7555
Month	February	0.63221	0.5245
Month	March	−1.45785	0.1433
Month	April	−2.90921	0.0028
Month	May	−3.10011	0.0021
Month	June	−3.13576	0.0023
Month	July	−3.0504	0.0024
Month	August	−3.03584	0.0026
Month	September	−3.01265	0.0020
Month	October	−2.99053	0.0018
Month	November	−1.99053	0.0363
Month	December	0	-
Pavement	Asphalt	−1.32337	0.0349
Pavement	Concrete	0	-

March are not statistically different than the number of subsurface freeze-thaw cycles in December, which is not surprising because these four months have similar weather patterns. Additionally, the numbers of subsurface freeze-thaw cycles in the months of April, May, June, July, August, September, October, and November are all statistically different than the number of subsurface freeze-thaw cycles in December. Pavement type is also a significant predictor of subsurface freeze-thaw cycles, and asphalt is expected to experience 1.32337 fewer freeze-thaw cycles per month than concrete, as shown in Table 4.4.

The R^2 value for this regression is 0.2656, which is fairly poor even for non-controlled experiments. Figure 4.11 shows the lack of equality between the predicted number of subsurface freeze-thaw cycles and the observed number of subsurface freeze-thaw cycles, confirming that the statistical analysis results are not accurate enough to be used in practice. The regression actually predicts negative freeze-thaw cycles for several stations and months and never predicts more than six freeze-thaw cycles for a single month. If the equation were accurate, all of the observations in Figure 4.11 would lie close to the line of equality.

The predicted number of freeze-thaw cycles shown in Figure 4.11 was found in each case by adding the appropriate estimates from Table 4.4. For example, to compute the predicted number of freeze-thaw cycles in February for station UT248, which has an elevation of 2,103 m (6900 ft) and a latitude of 40.63° and for which the pavement type is asphalt, the following terms were added together: the intercept estimate, the product of elevation in feet and the elevation estimate, the product of latitude in degrees and the latitude estimate, the estimate for February, and the estimate for asphalt. For station UT248, the predicted number of freeze-thaw cycles was therefore $(-7.91873) + (6900 \cdot 0.000324) + (40.63 \cdot 0.253717) + (0.63221) + (-1.32337) = 3.93$ freeze-thaw cycles. This station actually experienced 16 freeze-thaw cycles in the month of February.

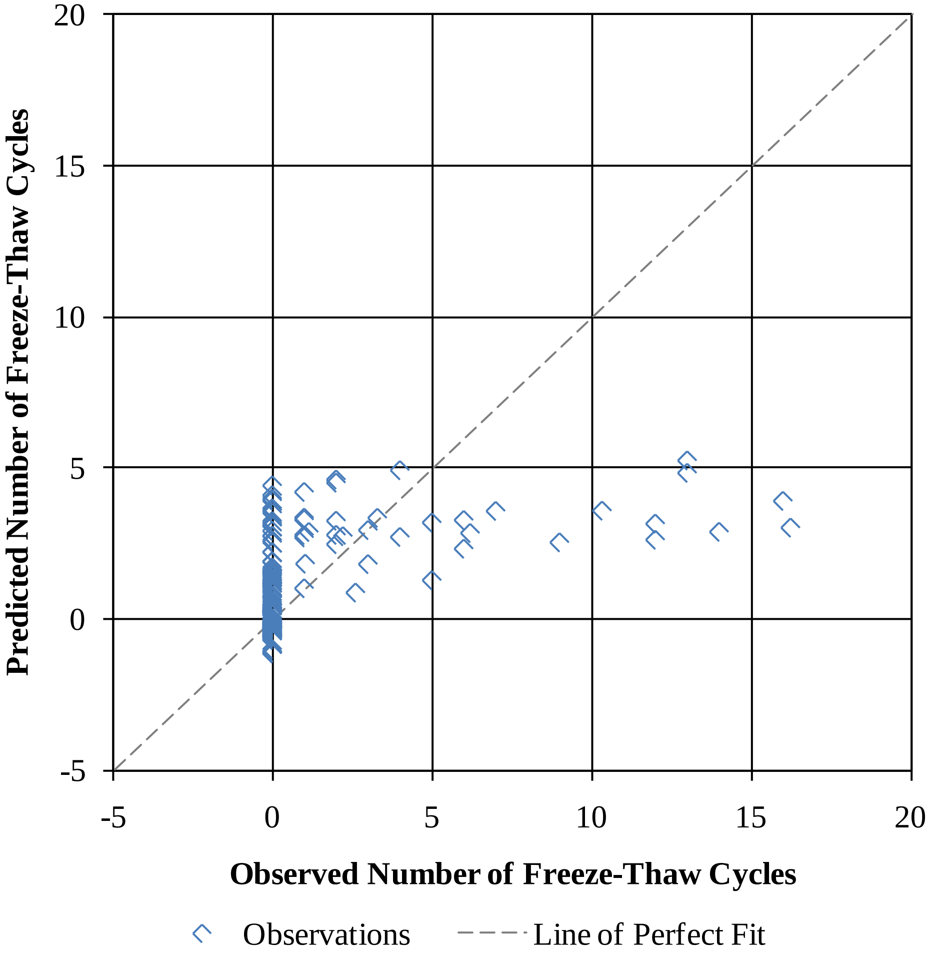

Figure 4.11 Predicted versus observed number of subsurface freeze-thaw cycles.

Because the regression equation does not accurately predict subsurface freeze-thaw cycles, an entirely different analysis must be conducted with different input variables. Data that were not available for this research but are likely necessary in estimating the number of freeze-thaw cycles under the pavement include pavement layer thicknesses, layer types, and layer moisture contents.

4.3 Finite-Difference Modeling

The simplified finite-difference model was used for two simulations. Both simulations started with 0°C (32°F) temperature gradients, and the air temperature in both simulations was increased to 1°C (34°F) for the duration of the simulation. The first simulation had no solar radiation, and the second simulation had 100 W/m^2 of solar radiation. The results of the first finite-difference simulation are shown in Figure 4.12 for the upper 0.1 m (0.3 ft) of the model pavement structure. After 1 minute, the surface temperature of the asphalt pavement increased by 0.23°C (0.41°F), and the surface temperature of the concrete pavement increased by 0.37°C (0.67°F). As time passed, the surface temperatures of both pavements approached the ambient air temperature, but concrete warmed up faster than asphalt.

The results of the second finite-difference simulation are shown in Figure 4.13, again for the upper 0.1 m (0.3 ft) of the model pavement structure. Initially, the asphalt and concrete pavements increased almost uniformly. After 60 minutes, both pavements had surface temperatures higher than the air temperature, but the concrete surface

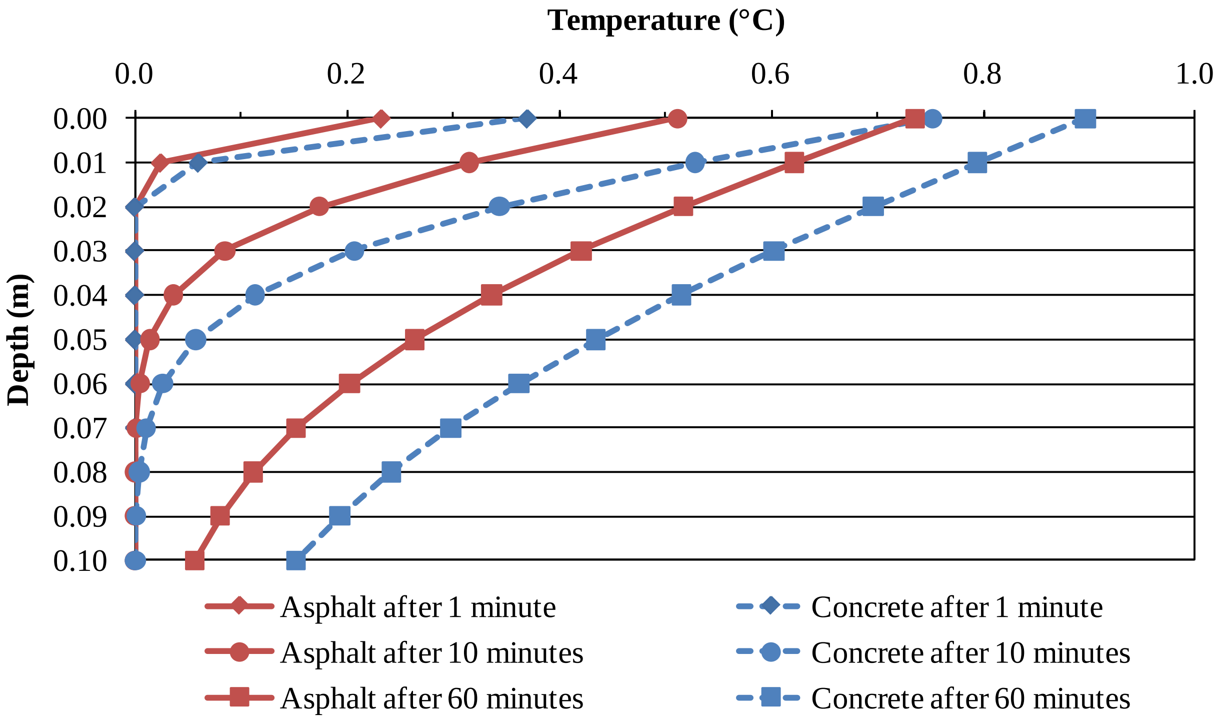

Figure 4.12 Temperature profiles reflecting a 1°C increase in air temperature.

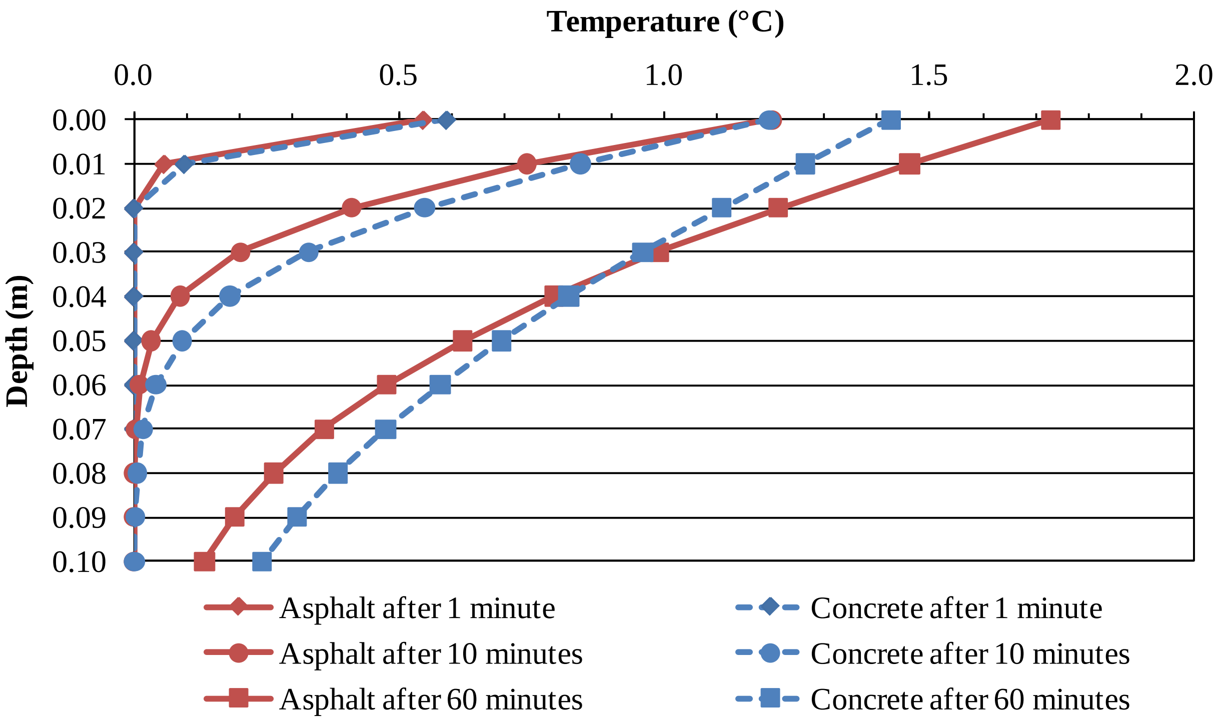

Figure 4.13 Temperature profiles reflecting a 1°C increase in air temperature and 100 W/m^2 incident radiation.

temperature was closer to the air temperature than the asphalt surface temperature. The asphalt pavement experienced higher surface temperatures because, having an albedo lower than that of the concrete pavement, it absorbed a larger percentage of incident radiation. Furthermore, even if the absorbed radiation for asphalt and concrete were equal, asphalt would still reach higher surface temperatures than concrete because asphalt has a lower specific heat.

This analysis shows that, for times with minimal incident radiation, concrete pavements tend to have higher surface temperatures than asphalt pavements, with all other factors constant. However, for scenarios with significant solar radiation, asphalt pavements tend to have higher surface temperatures than concrete pavements, again with all other factors constant. Since little or no solar radiation enters the pavement during the night and significant solar radiation enters the pavement during the day, the results of the finite-difference model are consistent with the results of the statistical analysis predicting pavement surface temperatures. That is, the results of both the statistical analyses and the finite-difference modeling show that, for times of low incident radiation (night), concrete has higher surface temperatures than asphalt, and, for times of high incident radiation (day), asphalt has higher surface temperatures than concrete.

4.4 Summary

The statistical analysis performed on pavement surface temperatures showed that, for near-freezing conditions, concrete pavements tend to have higher surface temperatures during *evening*, *night*, *early morning*, and *late morning*, while asphalt pavements tend to have higher surface temperatures for *early afternoon* and *late afternoon*. Although the analysis performed in this research indicates that the difference between surface temperatures for asphalt and concrete pavements is statistically significant, the difference is not practically important. The average of all air temperatures corresponding to the freezing point of asphalt pavements is exactly the same as the average of all air temperatures corresponding to the freezing point of concrete pavements, showing that, although asphalt is better in the afternoon and concrete is better for other times of the day with respect to winter maintenance, neither pavement type is better than the other, on average. From the standpoint of surface temperatures, asphalt and concrete are equally likely to collect snow or ice on their surfaces, and both pavements are expected to require equal amounts of winter maintenance, on average. Finite-difference analysis results confirmed that, for times of low incident radiation (night), concrete has higher surface temperatures than asphalt, and, for times of high incident radiation (day), asphalt has higher surface temperatures than concrete.

The regression equation predicting the number of subsurface freeze-thaw cycles from elevation, latitude, month, and pavement type provided estimates that did not correlate well with measured values. Consequently, an entirely different analysis must be conducted with different input variables. Data that were not available for this research but are likely necessary in estimating the number of freeze-thaw cycles under the pavement include pavement layer thicknesses, layer types, and layer moisture contents.

5.0 CONCLUSION

5.1 Summary

UDOT is responsible for the winter maintenance of 16,270 lane-miles of state highways. In 2009, UDOT spent approximately $22 million on snow removal, which includes identifying and removing snow and ice from the road surface through snowplows, sand, and salt. Because winter maintenance is so costly, UDOT personnel recognized the need for research on winter maintenance and asked researchers at Brigham Young University to determine whether asphalt or concrete pavements require more winter maintenance.

The first objective of this research was to determine which pavement type has higher surface temperatures in winter, holding everything else constant. Air temperature data and pavement surface temperature data from 31 ESSs (22 on asphalt roads and nine on concrete roads) in Utah were used to create a multiple linear regression that predicted pavement surface temperature given air temperature, time of day, and pavement type.

The second objective of this research was to compare the subsurface temperatures under asphalt and concrete pavements to determine the pavement type below which more freeze-thaw cycles of the underlying soil occur. To meet this objective, subsurface temperatures from the same 31 ESSs were used in a multiple linear regression that predicted subsurface freeze-thaw cycles given elevation, latitude, month, and pavement type.

Data for this research were acquired from two sources and had to be combined into a single database. Climatological data were acquired from the MesoWest website, and pavement type data were obtained from Google Maps. Twelve continuous months of data, primarily from the 2009 calendar year, were used for each station, and erroneous data were removed from the data set. Freeze-thaw cycles were counted at 45 cm (18 in.) underground, and the counts were scaled up based on the ratio of days in the month to days with data.

To predict the pavement surface temperatures, a multiple linear regression was performed with input parameters of pavement type, time period, and air temperature. Similarly, a multiple linear regression was performed to predict the number of subsurface freeze-thaw cycles, based on month, latitude, elevation, and pavement type. These parameters were chosen using the method of backward selection. A finite-difference model was created to model temperature gradients in asphalt and concrete pavements based on air temperature and incoming radiation.

5.2 Findings

The following two sections explain how the results of the statistical analyses and finite-difference modeling address the stated objectives of this research.

5.2.1 Pavement Surface Temperatures

The statistical analysis predicting pavement surface temperatures showed that, for near-freezing conditions, concrete pavements tend to have warmer surface temperatures for *evening*, *night*, *early morning*, and *late morning*, while asphalt pavements tend to have warmer surface temperatures for *early afternoon* and *late afternoon*. Although the analysis indicates that the difference between surface temperatures for asphalt and concrete pavements is statistically significant, the difference is not practically important. The average of all air temperatures corresponding to the freezing point of asphalt pavements is exactly the same as the average of all air temperatures corresponding to the freezing point of concrete pavements, showing that, although asphalt is better in the afternoon and concrete is better for other times of the day, neither pavement type is better, on average. From the standpoint of surface temperatures, asphalt and concrete are equally likely to collect snow or ice on their surfaces, and both pavements are expected to require equal amounts of winter maintenance, on average. Finite-difference analysis results confirmed that, for times of low incident radiation (night), concrete has higher surface temperatures than asphalt, and, for times of high incident radiation (day), asphalt has higher surface temperatures than concrete.

5.2.2 Subsurface Freeze-Thaw Cycles

The regression equation predicting the number of subsurface freeze-thaw cycles from elevation, latitude, month, and pavement type provided estimates that did not correlate well with measured values. Consequently, an entirely different analysis must be conducted with different input variables. Data that were not available for this research but are likely necessary in estimating the number of freeze-thaw cycles under the pavement include pavement layer thicknesses, layer types, and layer moisture contents.

5.3 Recommendations

When performing a life-cycle cost analysis to compare asphalt and concrete pavements in locations similar to the average condition evaluated in this research, UDOT engineers need not consider winter maintenance costs in the analysis because both asphalt and concrete are expected to require the same amount of winter maintenance, on average, in the state of Utah. Future research may be performed to investigate current winter maintenance expenditures for asphalt and concrete roads, including trends in deicer usage, for example. Further studies may also be warranted in particular locations in northern Utah more typical of canyon areas, where extreme climatic conditions may lead to different pavement behavior. Additionally, future research should be performed to develop an accurate and reliable method for predicting the number of subsurface freeze-thaw cycles under a pavement.

REFERENCES

1. Bernhard, L. (2009). "UDOT Maintenance Facts." <http://www.udot.utah.gov/main/uconowner.gf?n=2224298003431361897>. (June 24, 2010).

2. UDOT. (2010). "2010 Strategic Direction & Performance Measures." <http://www.udot.utah.gov/main/f?p=100:pg:0:::1:T,V:2374,>. (June 22, 2010).

3. Walls, J., III, and Smith, M. R. (1998). "Life-Cycle Cost Analysis in Pavement Design." Publication FHWA-SA-98-079. Federal Highway Administration, Washington, DC.

4. Sherif, A., and Hassan, Y. (2004). "Modelling Pavement Temperature for Winter Maintenance Operations." *Canadian Journal of Civil Engineering*, 31(2), 369-378.

5. American Society for Testing and Materials (ASTM). (2010). "ASTM D7228 - 06a Standard Test Method for Prediction of Asphalt-Bound Pavement Layer Temperatures." *Annual Book of ASTM Standards*, 04.03, West Conshohocken, PA.

6. Solaimanian, M., and Kennedy, T. W. (1993). "Predicting Maximum Pavement Surface Temperature Using Maximum Air Temperature and Hourly Solar Radiation." *Transportation Research Record*, 1417, 1-11.

7. McPherson, T. (2004). "County Drivers Feel the Effects of Increase in Deteriorating Roads." <http://www.heraldextra.com/news/local/article_cc2aae62-7ff4-53b2-9064-7277c031984b.html>. (August 3, 2010).

8. Jackson, N., and Puccinelli, J. (2006). "Long-Term Pavement Performance (LTPP) Data Analysis Support: National Pooled Fund Study TPF-5(013): Effects of Multiple Freeze Cycles and Deep Frost Penetration on Pavement Performance and Cost." Publication FHWA-HRT-06-121. Federal Highway Administration, Washington, DC.

9. Puccinelli, J., and Jackson, N. (2007). "Development of Pavement Performance Models to Account for Frost Effects and Their Application to Mechanistic-

Empirical Design Guide Calibration." *Transportation Research Record*, 1990, 95-101.

10. Yoder, E. J., and Witczak, M. W. (1975). *Principles of Pavement Design*, John Wiley & Sons, Inc., Hoboken, NJ.

11. Jestor, R. N. (1997). *Progress of Superpave (Superior Performing Asphalt Pavement): Evaluation and Implementation*, American Society for Testing and Materials, West Conshohocken, PA.

12. Hardin, J. C. (1995). *Physical Properties of Asphalt Cement Binders*, ASTM International, Philadelphia, PA.

13. Monismith, C. L., Secor, G. A., and Secor, K. E. (1965). "Temperature Induced Stresses and Deformations in Asphalt Concrete." *Proc., Association of Asphalt Paving Technologists*, 248-285.

14. Westergaard, H. M. (1927). "Analysis of Stresses in Concrete Pavements Due to Variations of Temperature." *Proc., Highway Research Board*, 6, 201-215.

15. Armaghani, J. M., Larsen, T. J., and Smith, L. L. (1987). "Temperature Response of Concrete Pavements." *Transportation Research Record*, 1121, 23-33.

16. Pomerantz, M., Pon, B., Akbari, H., and Chang, S. C. (2000). "The Effect of Pavements' Temperatures on Air Temperatures in Large Cities." Lawrence Berkeley National Laboratory, Berkeley, CA, 1-22.

17. Asaeda, T., Ca, V. T., and Wake, A. (1996). "Heat Storage of Pavement and Its Effect on the Lower Atmosphere." *Atmospheric Environment*, 30(3), 413-427.

18. University of Utah. (2010). "MesoWest." <http://mesowest.utah.edu/>. (May 5, 2010).

19. FHWA (2010). "Clarus System." <http://www.clarus-system.com/ShowMetadata.jsp?file=sensorType.csv>. (May 4, 2010).

20. Boselly, S. E., Doore, G. S., and Ernst, D. D. (1993). "Road Weather Information Systems Volume 2: Implementation Guide." Publication SHRP-H-351. Strategic Highway Research Program, Federal Highway Administration, Washington, DC .

21. Manfredi, J., Walters, T., Wilke, G., Osborne, L., Hart, R., Incrocci, T., and Schmitt, T. (2005). "Road Weather Information System Environmental Sensor Station Siting Guidelines." Publication FHWA-HOP-05-026. Federal Highway Administration, Washington, DC.

22. Federal Highway Administration (FHWA). (2002). "An Introduction to Standards for Road Weather Information Systems (RWIS): Siting Standards, Calibration Standards, Communications Standards." Publication FHWA-OP-02-079. Federal Highway Administration, Washington, DC.

23. Utah Department of Transportation (UDOT). (2009). "CommuterLink." <http://commuterlink.utah.gov/>. (June 22, 2010).

24. Quixote Transportation Technologies, Inc. (QTT). (2008a). "Atmospheric Sensors." <http://www.qttinc.com/pages/atmosphinstra.html>. (June 29, 2010).

25. Vaisala. (2010). "Solar Radiation Sensors." <http://www.vaisala.com/weather/products/solarradiation.html>. (June 29, 2010).

26. QTT. (2008b). "Pavement Sensors." < http://www.qttinc.com/pages/fp2000.html>. (June 29, 2010).

27. Green, J. (2008). "Intelligent Road Sensor." <http://atmoswiki.aero.und.edu/atmos/535/projects/lufft_intelligent_road_sensor>. (July 19, 2010).

28. Google. (2010). "Google Maps." <http://maps.google.com/>. (June 22, 2010).

29. Crouch, C. J., Crouch, D. B., Maclin, R. M., and Polumetla, A. (2005). "Automatic Detection of RWIS Sensor Malfunctions (Phase I)." University of Minnesota Duluth, Duluth, MN, 1-43.

30. U.S. Naval Observatory (USNO). (2010). "Sun or Moon Rise/Set Table for One Year: U.S. Cities and Towns." <http://www.usno.navy.mil/USNO/astronomical-applications/data-services/rs-one-year-us>. (June 22, 2010).

31. Ramsey, F. L., and Schafer, D. W. (2002). *The Statistical Sleuth*, Duxbury, Pacific Grove, CA.

32. Ryan, T. P. (2007). *Modern Engineering Statistics*, John Wiley & Sons, Inc., Hoboken, NJ.

33. Hermansson, Å. (2004). "Mathematical Model for Paved Surface Summer and Winter Temperature: Comparison of Calculated and Measured Temperatures." *Cold Regions Science and Technology*, 40(1-2), 1-17.

APPENDIX: Division of Data into Time Periods Based on Road Temperatures

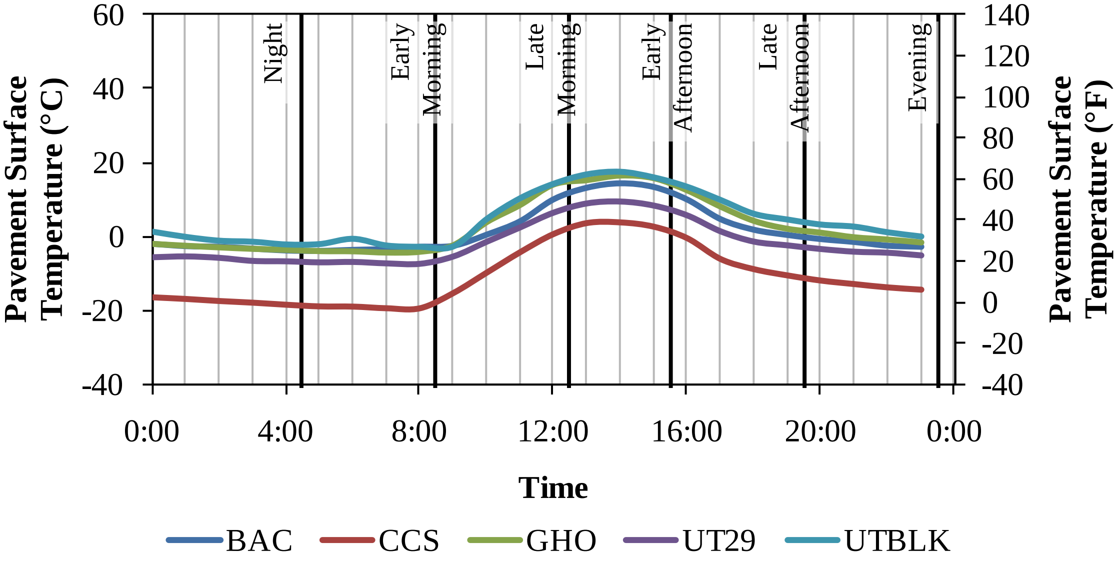

Figure A.1 January 15th road temperatures for each time period.

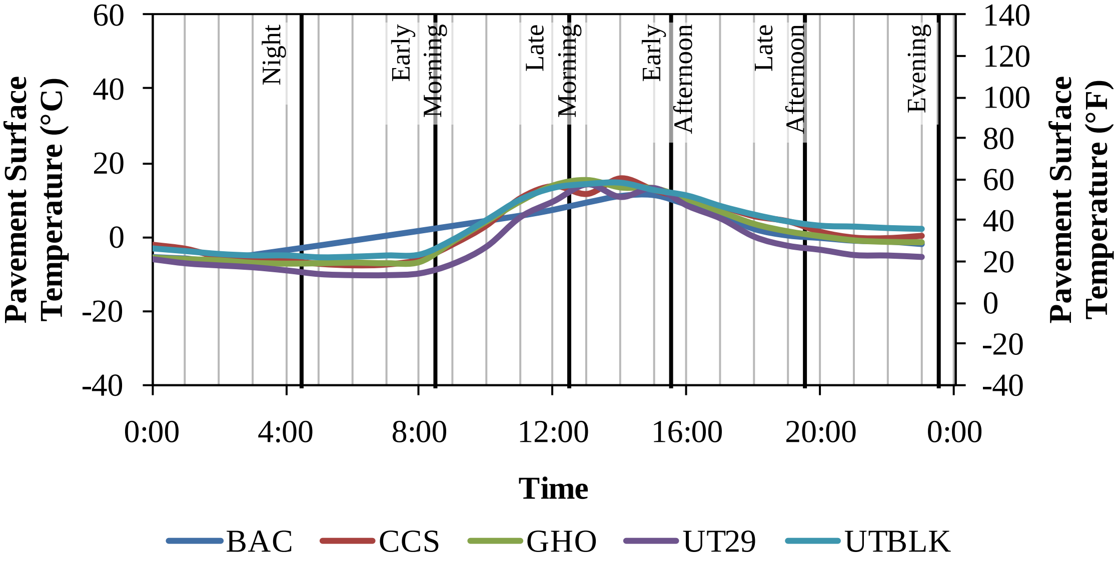

Figure A.2 February 15th road temperatures for each time period.

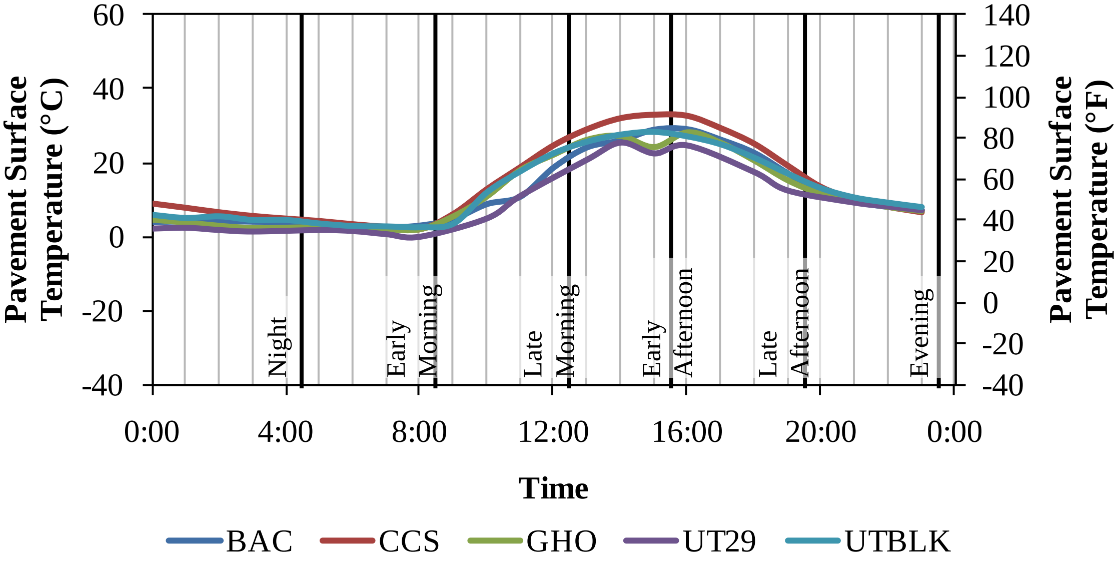

Figure A.3 March 15th road temperatures for each time period.

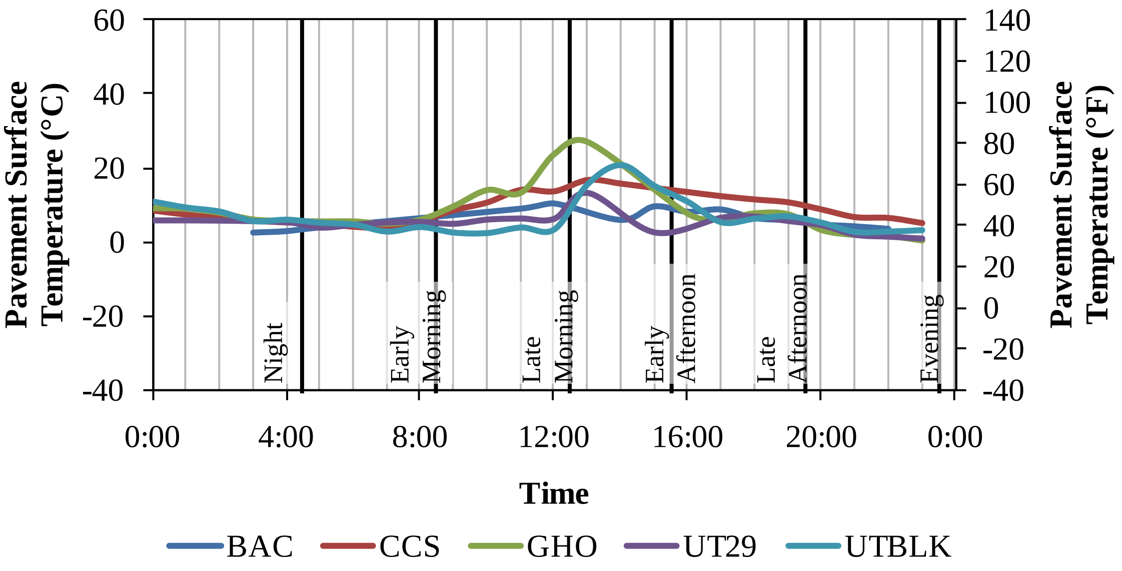

Figure A.4 April 15th road temperatures for each time period.

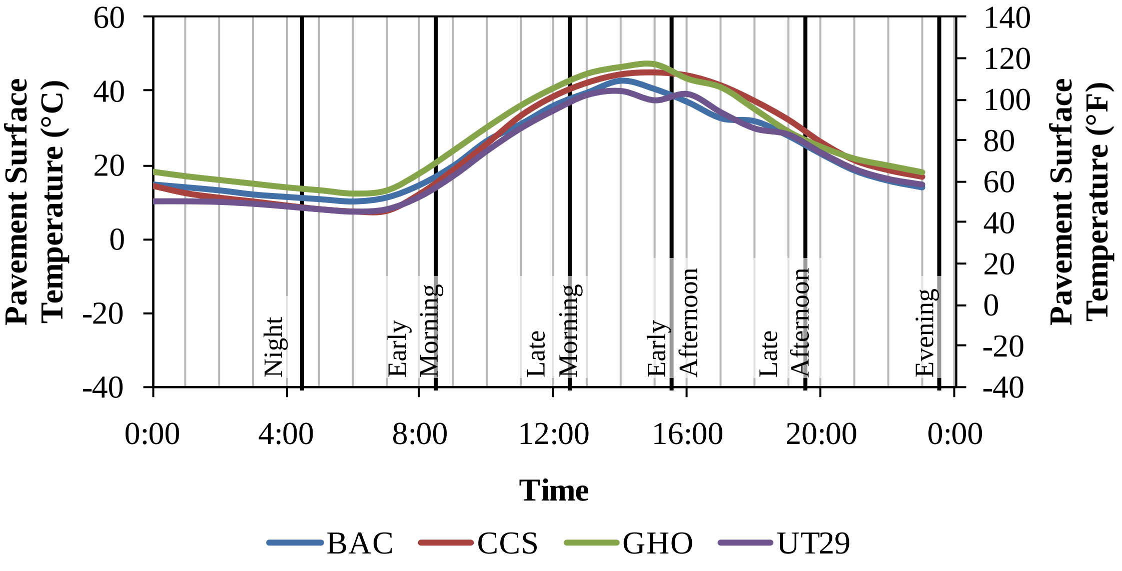

Figure A.5 May 15th road temperatures for each time period.

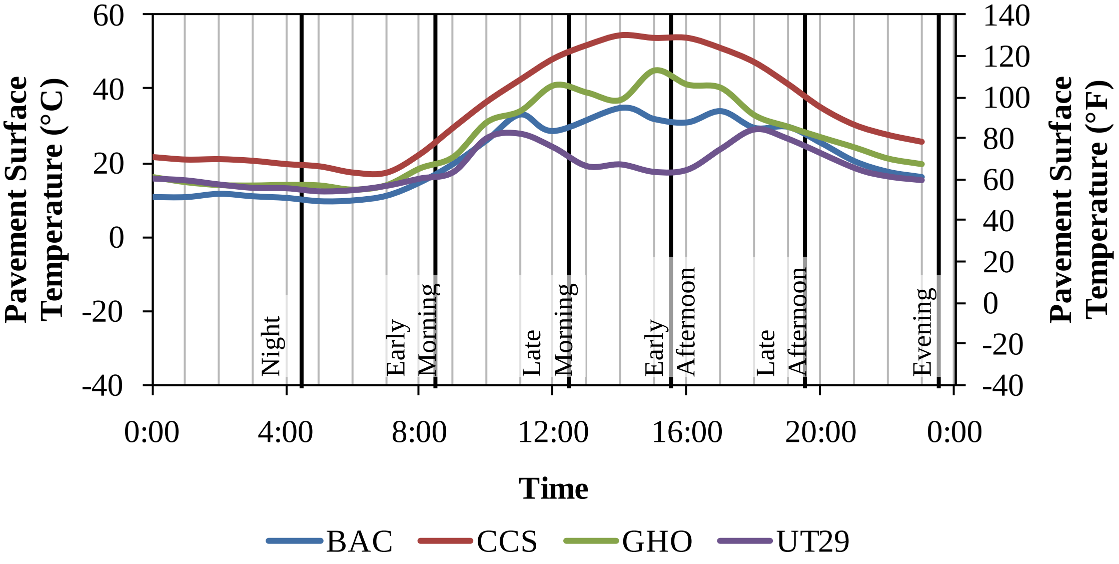

Figure A.6 June 15th road temperatures for each time period.

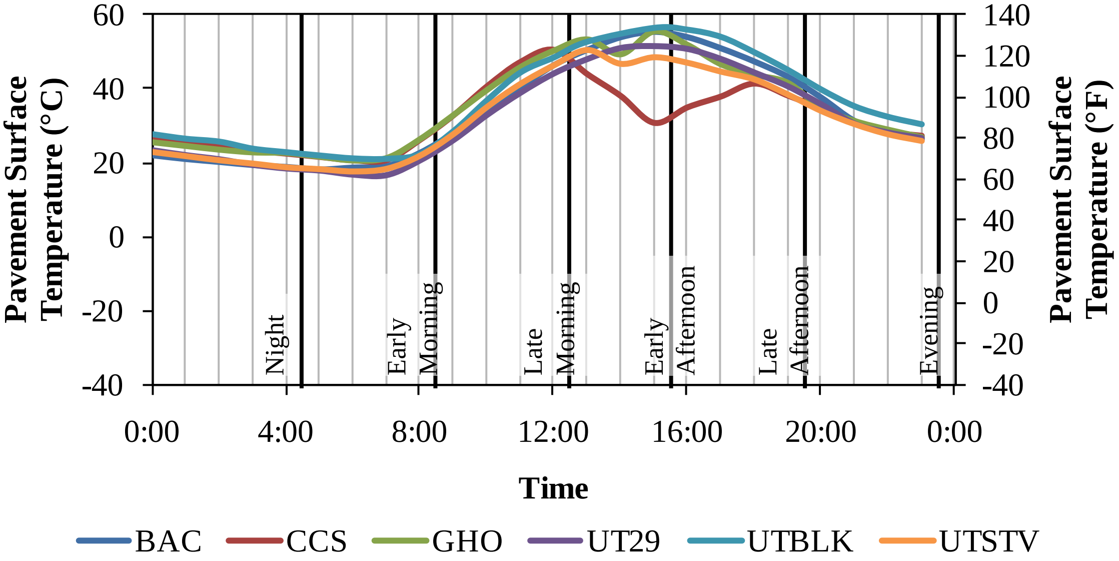

Figure A.7 July 15th road temperatures for each time period.

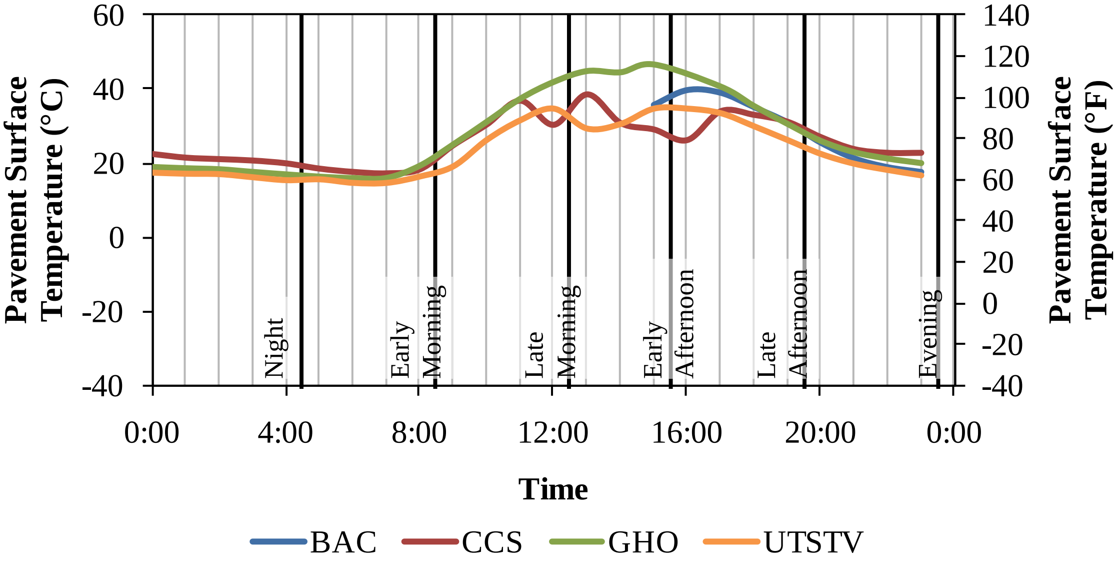

Figure A.8 August 15th road temperatures for each time period.

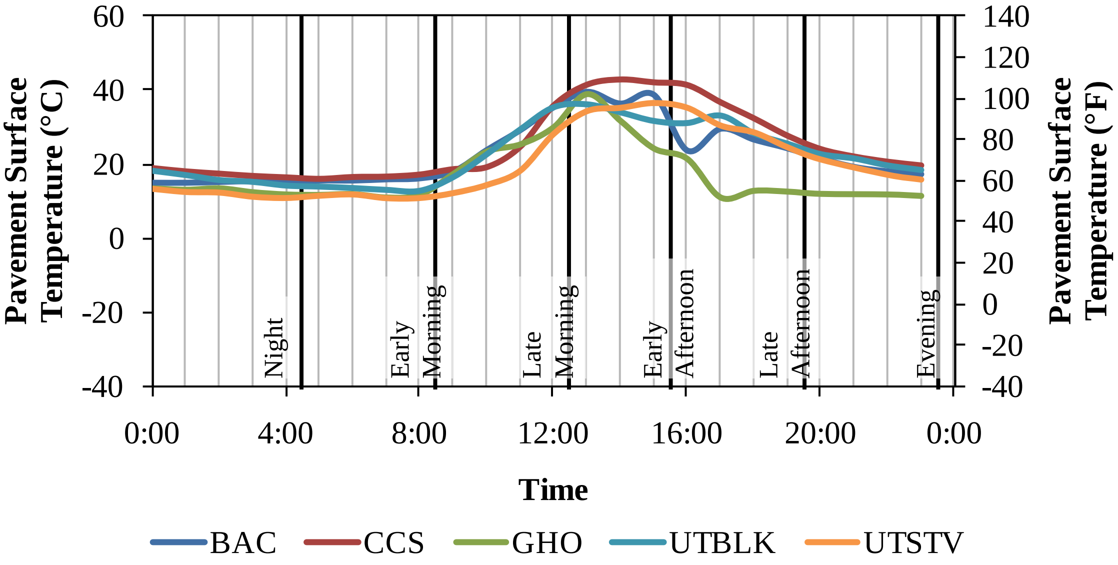

Figure A.9 September 15th road temperatures for each time period.

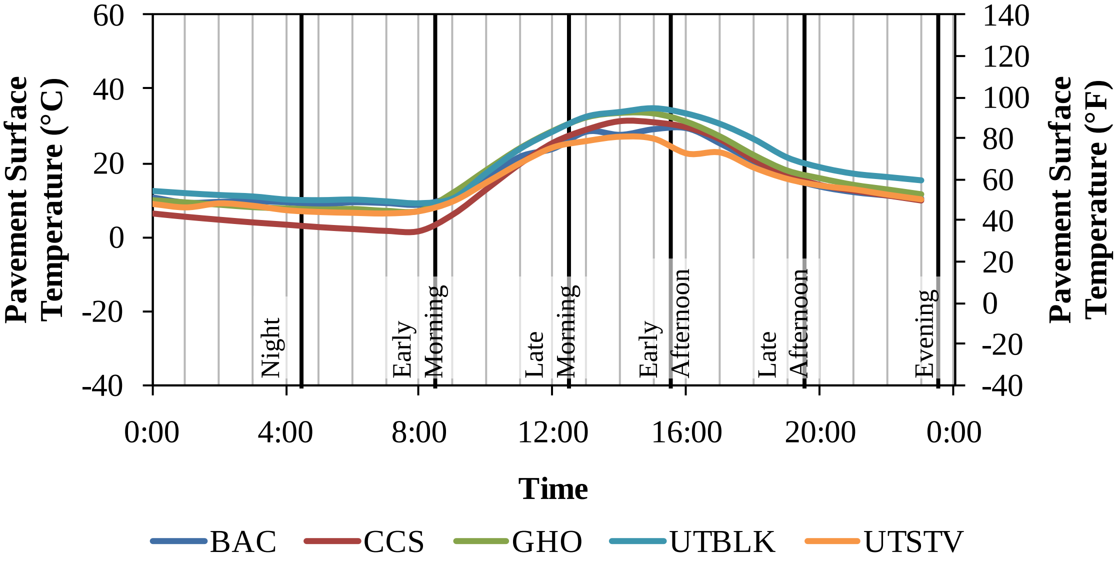

Figure A.10 October 15th road temperatures for each time period.

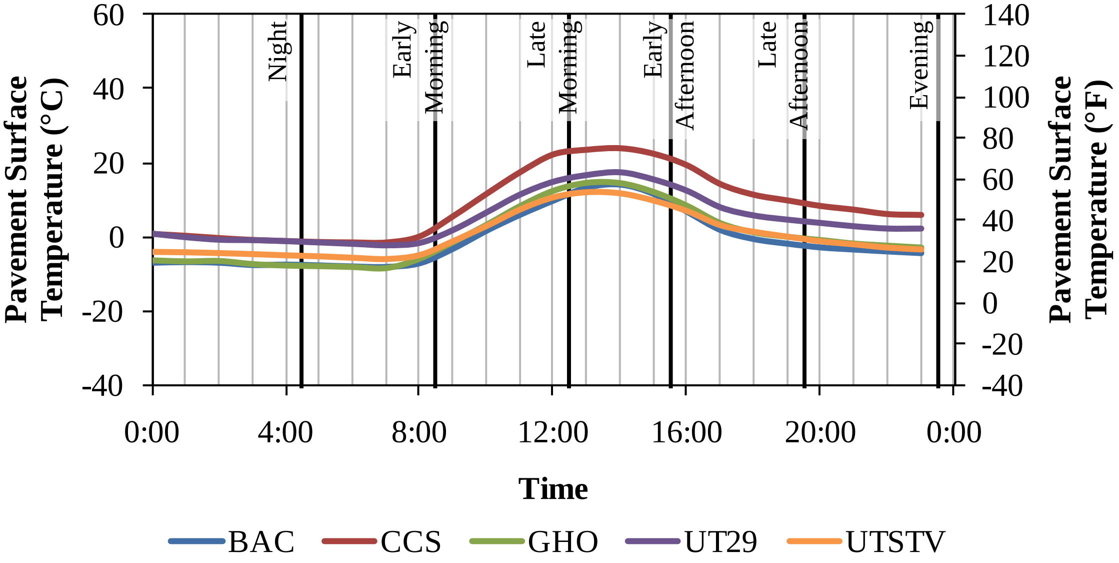

Figure A.11 November 15th road temperatures for each time period.

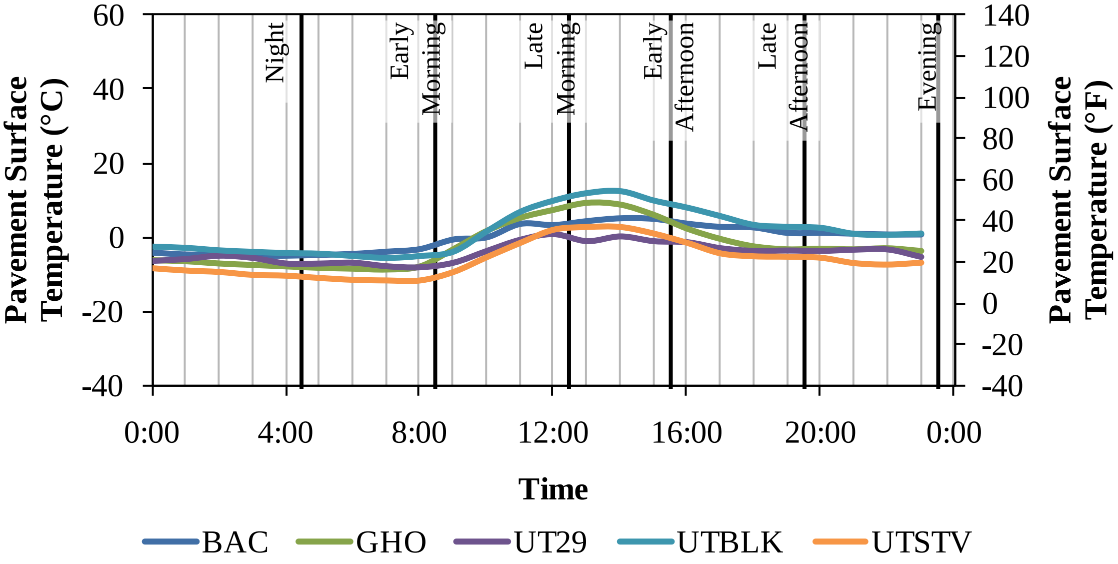

Figure A.12 December 15th road temperatures for each time period.